Concatenated Channel Coding and Orthogonal Space-Time Block Coding for MIMO Systems: Antenna Selection and Performance Bounds

Xiangnian Zeng

A Thesis

in

The Department

of

Electrical and Computer Engineering

Presented in Partial Fulfillment of the Requirements

for the Degree of Master of Applied Science

Concordia University

Montreal, Quebec, Canada

August 2004

Your file Votre référence
ISBN: 0-612-94717-3
Our file Notre référence
ISBN: 0-612-94717-3

Abstract

Concatenated Channel Coding and Orthogonal Space-Time Block Coding for MIMO Systems: Antenna Selection and Performance Bounds

Xiangnian Zeng

In this thesis, we study the performance of orthogonal space-time block codes (STBCs) over Rayleigh fading channels with receive antenna selection. For a given number of receive antennas M, we assume that the receiver uses the best L of the available M antennas, where, typically, $L \leq M$. The selected antennas are those that maximize the instantaneous received signal-to-noise ratio (SNR). In our analysis we consider 1) orthogonal STBCs only, and 2) concatenated channel coding with STBCs. For both coding schemes, we consider uncorrelated and spatially correlated fading channels. We derive explicit upper bounds on the bit error rate (BER) for the above schemes with antenna selection. We also derive exact analytical results for special cases. Our results show that the diversity order, with antenna selection, is maintained as that of the full complexity system, i.e., when the receiver uses all the available antennas, whereas the deterioration in SNR due to receive antenna selection is upper bounded by $10\log_{10}(M/L)$ dB. We also present numerous examples that validate our results.

Dedicated to my dearest mother, father, and sister.....

Acknowledgments

First of all, my sincere appreciation goes to my academic supervisor Dr. Ali Ghrayeb who has offered me invaluable support, constructive guidance and helpful discussion throughout my thesis research. I am grateful for his patience and kindness in answering my questions and revising my submitted reports. Without his continuous encouragement and stimulating suggestions I would not have completed my thesis.

I would like to thank the committee members Dr. M. R. Soleymani, Dr. X. Zhou and Dr. W. Hamouda. Their comments make the presentation of this thesis more clear.

I would also like to thank Chuanxiu Huang, Hao Shen, Mohamed Abou-Khousa and Abdollah Sanei in our research group. It is because of their help that I overcame some technical problems when my knowledge to solve some problem had been exhausted. I want to thank all the people who help me throughout my study at Concordia University.

Finally, I would like to thank my parents for their love, trust and encouragement throughout all the two years. Without their support, it would have been impossible for me to accomplish what I have accomplished.

Contents

List of Figures

List of Tables

Chapter 1

Introduction

1.1 MIMO Systems

Multiple-input-multiple-output (MIMO) wireless systems are those that have multiple antenna elements at both the transmitter and receiver. They are now being used for third-generation cellular systems (W-CDMA) and are discussed for future high-performance modes of the IEEE 802.11 standard for wireless local area network. The multiple antennas in MIMO systems can be exploited in two ways. One is the use of multiple antennas to increase capacity. This can effectively meet the rapidly increased capacity demands driven by cellular mobile, Internet and multimedia services in wireless communication. Several different data streams can be transmitted parallel from the different transmit antennas. At the receiver, multiple receive antennas are used to separate the different data streams. Thus, a drastic increase in the channel capacity can be achieved through MIMO systems, as shown by Telatar [1],

and Foschini and Gans [2].

The other use of MIMO systems is to create antenna diversity. The challenge of achieving reliable data transmission over wireless links stems from the fact that, in a wireless environment, unlike other applications, achieving reliable communication becomes much more difficult due to the possibility that received signals from multipaths may add destructively, which, consequently, results in a serious performance degradation. It has been shown that a key technique for achieving reliable communication over wireless links is to introduce antenna diversity into the system.

Antenna diversity is achieved by employing spatially separated antennas at the transmitter and/or at the receiver. The separation requirements vary with antenna height, propagation environment and frequency so that the subchannels are uncorrelated. At the receiver, multiple replicas of the transmitted signals are available, all carrying the same information but with small correlation in fading statistics since they transmit via different subchannels. The basic idea of antenna diversity is that, if two or more independent subchannels are available, these subchannels will fade in an uncorrelated manner, e.g., some subchannels are severely faded while others are less attenuated. This means that the probability of all the subchannels simultaneously fade below a given level is much lower than the probability of any individual subchannel fades below that level. Thus, a proper combination of the signals from different subchannels results in greatly reduced severity of fading, and correspondingly, improved reliability of transmission. Another advantage of antenna diversity compared with time and frequency diversity is that, antenna diversity does not induce any loss

in bandwidth efficiency. This property is very attractive for future high data rate wireless communications.

1.2 Space-Time Codes

1.2.1 Development of Space-Time Codes

Inspired by the promised increase in capacity, a large number of papers have been published recently on the use of antenna diversity for achieving reliable communication over wireless links. These include the early work by Guey, *et al.* [3] in which they consider signal design techniques that exploit the diversity provided by employing multiple antennas at the transmitter. Then Tarokh, *et al.* introduced in 1998 [4] the class of space-time trellis codes (STTCs), by jointly designing the error control coding, modulation, transmit and receive diversity. STTCs are very efficient for systems with multiple transmit and receive antennas. The encoding and decoding complexity is comparable to that of conventional trellis codes.

A few months later, in [5], Alamouti introduced a very simple, and yet efficient, scheme which involves using two transmit antennas at the base station (BS) and one receive antenna at the other end of the downlink. A simple decoding algorithm based on a linear receiver was introduced for this scheme, which can be extended for an arbitrary number of receive antennas. This scheme is significantly less complex than STTCs using two transmit antennas, although there is a loss in performance. Motivated by the simplicity of the Alamouti scheme, Tarokh, *et al.* [6] generalized

that scheme to an arbitrary number of transmit antennas, resulting in the so-called space-time block codes (STBCs). Since the discovery of space-time codes, many papers have appeared in the literature in which various space-time coding schemes were considered in an effort to maximize the diversity order and coding gain for a given number of transmit and receive antennas, see [7]−[11] and the references therein.

Despite the low complexity STBCs enjoy, such codes do not provide any coding gain, unlike the case for STTCs. Therefore, a STBC, if considered, may need to be combined with an outer channel coding scheme in order to provide such coding gains. To this end, a few papers have appeared recently in the literature in which various coding schemes concatenated with STBCs were considered, including [12]−[17], among others. It was observed in these works that substantial coding gains can be achieved. In some cases, it was demonstrated that a STBC used in conjunction with an outer channel code can be superior, in terms of performance, to a STTC at even a lower complexity [17]. In most of these works, however, the conclusions were based on computer simulations and no analytical performance analysis was performed on BER.

1.2.2 Space-Time Block Codes

In general, a STBC is defined by an $N \times p$ transmission matrix $\mathbf{X}_N$. Here N represents the number of transmit antennas and p represents the number of time periods for transmission of one block of coded symbols. The transmission matrix describes the relationship between the original transmitted signal $x_1, x_2, \ldots, x_k$ and the signal

replicas artificially created at the transmitter for transmission over various diversity channels. Each entry of the matrix is constituted of linear combinations of the k input symbols $x_1, x_2, \ldots, x_k$ and their conjugates $x_1^*, x_2^*, \ldots, x_k^*$.

$$\mathbf{X}_N = \begin{bmatrix} g_{11} & g_{12} & \cdots & g_{1p} \\ g_{21} & g_{22} & \cdots & g_{2p} \\ \vdots & \vdots & \ddots & \vdots \\ g_{N1} & g_{N2} & \cdots & g_{Np} \end{bmatrix}$$

The encoding diagram is shown in Fig. 1.1. Assume the signal constellation consists of 2^m points. At each encoding operation, a block of km information bits are mapped into signal constellation to select k modulated signals, where each group of m bits selects a constellation signal. The k modulated signals are encoded by a space-time block encoder to generate N parallel signal sequences of length p according to the transmission matrix $\mathbf{X}_N$. These sequences are transmitted through N transmit antennas simultaneously in p time periods. So, the code rate of STBCs is k/p.

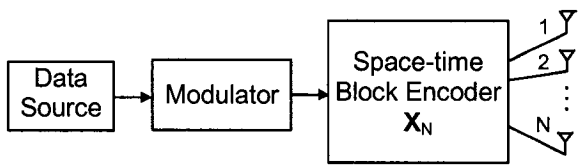

Figure 1.1: Space-time block encoder.

In order to achieve the full transmit diversity, the transmission matrix $\mathbf{X}_N$ is

constructed based on orthogonal design such that [6]

$$\mathbf{X}_N \cdot \mathbf{X}_N^H = c\left(|x_1|^2 + |x_2|^2 + \cdots + |x_k|^2\right)\mathbf{I}_N$$

where c is a constant, $\mathbf{X}_N^H$ is the Hermitian of $\mathbf{X}_N$ and $\mathbf{I}_N$ is an $N \times N$ identity matrix. This means that in each block, the signal sequences from any two transmit antennas are orthogonal. The orthogonality enables to achieve the full transmit diversity for a given number of transmit antennas. In additional, it allows the receiver to decouple the signals transmitted from different antennas and consequently, a simple maximum likelihood decoding, based only on linear processing of the received signals.

1.2.3 Alamouti Scheme

We use the Alamouti scheme, which is the STBC for two transmit antennas with one receive antenna to show the decoding procedure of STBC. This can be readily extended to an arbitrary number of receive antennas. The transmission matrix for the Alamouti scheme is as follows.

$$\mathbf{X}_2 = \begin{bmatrix} x_1 & -x_2^* \\ x_2 & x_1^* \end{bmatrix}$$

Denote $\alpha_i, i = 1, 2$ as the fading coefficient between the i^{th} transmit antenna and receive antenna. Assume the fading coefficients are constant across the corresponding two consecutive time slots. Then the received signal at the first and second time slot

can be represented as

$$\begin{aligned} y_1 &= \alpha_1 x_1 + \alpha_2 x_2 + w_1 \\ y_2 &= -\alpha_1 x_2^* + \alpha_2 x_1^* + w_2 \end{aligned}$$

where w_1 and w_2 are independent noise samples added by the receive antenna in each time slot. In order to extract signal x_1 and x_2, the received signal y_1 and y_2 are combined according to

$$\begin{aligned} \tilde{x}_1 &= \alpha_1^* y_1 + \alpha_2 y_2^* \\ &= \left(|\alpha_1|^2 + |\alpha_2|^2\right) x_1 + \alpha_1^* w_1 + \alpha_2 w_2^* \end{aligned}$$

$$\begin{aligned} \tilde{x}_2 &= \alpha_2^* y_1 - \alpha_1 y_2^* \\ &= \left(|\alpha_1|^2 + |\alpha_2|^2\right) x_2 + \alpha_2^* w_1 - \alpha_1 w_2^*. \end{aligned}$$

The decision statistics $\tilde{x}_1$ and $\tilde{x}_2$ are then passed to the maximum-likelihood (ML) detector to determine the most likely transmitted symbols.

Now, let us assume binary phase-shift keying (BPSK) modulation scheme. The decision statistics can be reduced to the real part of the signals out of the combiner,

i.e.

$$\begin{aligned}\tilde{x}_1 &= \mathrm{Re}\left\{\alpha_1^* y_1 + \alpha_2 y_2^*\right\} \\ &= \left(|\alpha_1|^2 + |\alpha_2|^2\right) x_1 \\ &\quad + \mathrm{Re}\left\{\alpha_1\right\}\mathrm{Re}\left\{w_1\right\} + \mathrm{Im}\left\{\alpha_1\right\}\mathrm{Im}\left\{w_1\right\} + \mathrm{Re}\left\{\alpha_2\right\}\mathrm{Re}\left\{w_2\right\} + \mathrm{Im}\left\{\alpha_2\right\}\mathrm{Im}\left\{w_2\right\}.\end{aligned}$$

Let us model the noise w_1 and w_2 as independent samples of a zero-mean complex Gaussian random variable (rv) with variance $N_0/2$ per dimension. Assume symbol $x_1 = 1$ is transmitted. Then, $\tilde{x}_1$ is a Gaussian rv with mean $\left(|\alpha_1|^2 + |\alpha_2|^2\right)$ and variance $\frac{N_0}{2}\left(|\alpha_1|^2 + |\alpha_2|^2\right)$. According to the ML detector, the conditional BER conditioned on fading coefficients can be represented as

$$P_b(e \mid \boldsymbol{\alpha}) = Q\left(\sqrt{2\frac{E_s}{N_0}\left(|\alpha_1|^2 + |\alpha_2|^2\right)}\right), \tag{1.1}$$

where $Q(x)$ is the area under the tail of the Gaussian PDF and defined as

$$Q(x) = \frac{1}{\sqrt{2\pi}}\int_x^\infty e^{-t^2/2}dt, \qquad x \geq 0,$$

$\boldsymbol{\alpha} = \{\alpha_1, \alpha_2\}$, and E_s is the energy of the symbol transmitted from each transmit antenna. This can be generalized to any STBC with multiple receive antennas as we will show later in Chapter 2 expression (2.2).

1.3 Antenna Selection for MIMO Systems

One of the drawbacks of using multiple antennas is the associated complexity and the increased cost. While additional antenna elements are usually inexpensive, and the additional digital signal processing becomes even cheaper, the RF chains, which include low-noise amplifiers, downconverters, and analog-to-digital converters, are expensive and do not follow Moore's low. So the complexity that arises from using a separate RF chain for every employed antenna results in a significant increase in the implementation cost. In addition, in some cases, it may be prohibitively complex to use many RF chains, such as the case in mobile phones. With this motivation, antenna selection has been introduced recently as a means to alleviate this complexity, while exploiting the diversity provided by the transmit and receive antennas [18]−[35]. The idea behind antenna selection centers around using only a subset of the available antennas in MIMO systems. The implication of this selection is that the number of RF chains required is reduced to as few as the number of selected antennas, and thereby the deployment of MIMO systems would become less expensive and more feasible.

Here we emphasize that the conventional topic of selection diversity improvement and maximal ratio combining improvement for single-input-multiple-output (SIMO) Rayleigh fading channel has already been well studied in [36]. But it is definitely different from our topic of antenna selection for MIMO systems. For example, the average signal-to-noise ratio (SNR) improvement offered by choosing one out of M

available receive antennas compared with one out of one receive antenna is shown to be $\sum_{k=1}^{M} \frac{1}{k}$ for SIMO systems [36]. The derivation is quite straightforward due to the fact that there is only one transmit antenna. So, the signal envelop picked up by each receive antenna is with Rayleigh distribution, which is in the form of exponential expression. It is this exponential distribution that makes the antenna selection for SIMO systems a mathematically tractable topic. However, in the case of MIMO systems, such like that STBCs are used, the signal energy picked up by each receive antenna is Chi-square distributed, which is in the form of gamma distribution and consequently make the analysis quite difficult as will be shown in the later chapters. So, recently, antenna selection at the transmitter and the receiver under certain channel conditions has been considered for STTCs and STBCs extensively.

In [18], the authors consider the joint transmit and receive antenna selection based on the second order channel statistics, which is assumed to be available to the transmitter. The authors in [19] consider antenna selection for low rank matrix channels where selection is performed only at the transmitter. In [20], antenna selection is considered only at the transmitter with the assumption that the channel statistics are available to the transmitter. In [21], the authors show that, for full-rank STTCs over quasi-static fading channels, the diversity order is the same as that of the full-complexity system. The authors in [22] consider receive antenna selection for STTCs over fully interleaved channels. It was shown that the resulting diversity order with antenna selection is dependent upon the number of selected antennas and not on the number of available antennas, i.e., the diversity order is not maintained with antenna

selection. In [23], Molisch *et al.* studied the effect of antenna selection from a channel capacity perspective. It was shown that only a small loss in capacity is suffered when the receiver uses a good subset of the available receive antennas. Other work related to antenna selection for STTCs can be found in [24]−[30].

In [31]−[33], the authors consider antenna selection for STBCs at the transmitter. They show that the performance is improved by increasing the number of transmit antennas while keeping the number of selected antennas fixed. In [34], antenna selection is considered at the transmitter (with the full knowledge of the channel statistics) or at the receiver for orthogonal STBCs with particular emphasis on the Alamouti scheme [5]. In their analysis, they adopt a selection criterion that maximizes the channel Frobenius-norm and, accordingly, derive expressions for the improvement in the average signal-to-noise ratio (SNR) and outage capacity. They use outage probability analysis to argue that the spatial diversity, when the underlying space-time code is orthogonal, is maintained with antenna selection. In [35], the authors consider the concatenation of an outer convolutional code (CC) and a STBC. It was demonstrated that the diversity order is maintained with antenna selection.

In [37], the authors propose a new scheme that involves using hybrid selection/maximal-ratio transmission where the transmitter uses a good subset of the available antennas and the receiver uses maximum-ratio combining. They investigate this scheme in terms of signal-to-noise ratio (SNR), bit error rate, and capacity. They demonstrate the effectiveness of their scheme relative to already existing schemes. The same

scheme was also treated in [38] but when the transmitter selects the best single antenna. Other schemes that use hybrid selection/maximal-ratio combining were also considered in [39]−[42]. A nice overview of antenna selection for MIMO systems can be found in [43].

In most of the above work on antenna selection, it has been assumed that the subchannels fade independently. The implication of this assumption is that the adjacent antenna elements are assumed to be placed far enough from each other so that they experience completely different fading. However, it may be difficult to satisfy this condition in practice, particularly when the wireless device is relatively small where it is not possible to keep enough distance between adjacent antennas. Also, the assumption of independent fading no longer holds in an environment where scattering is not rich. In [44] and [45], the authors present a model for a correlated Rayleigh fading channel, and study the effect of correlation from a channel capacity perspective. In [46] and [47], the error probability of space-time codes in correlated fading channels is studied. Furthermore, in [48], the authors consider antenna selection for space-time trellis codes over correlated fading channels.

1.4 Thesis Outline

In this thesis, we present a comprehensive performance analysis of space-time block coded MIMO system with receive antenna selection. In the following chapters, we analysis the effect of receive antenna selection for four kinds of MIMO system models

respectively. In each chapter, we make the system model a little more complex or practical than that in the previous chapter, which enables us to study the topic step by step.

In Chapter 2, we consider the simplest MIMO system employing a STBC over independent flat Rayleigh fading channel.

In Chapter 3, we improve the performance of the system studied in Chapter 1 by concatenating an outer channel code with STBC. We consider the convolutional code (CC) and trellis code modulation (TCM) as an outer channel code, respectively.

In Chapter 4, to make the system model more practical, we consider the MIMO system in Chapters 1 and 2 over space correlated flat Rayleigh fading channel.

In Chapter 5, conclusions are made and directions for future work are suggested.

1.5 Thesis Contribution

This thesis presents the BER performance bounds for receive antenna selection of MIMO systems employing STBCs over flat Rayleigh fading channel based on the existing coding, decoding and antenna selection algorithm. The main contributions of the thesis are listed as follows:

- For STBC-only systems over independent fading channels, we present two general upper bounds for any N, M and L; a tighter upper bound for any N, and M when $L = 1$; and exact analysis for the Alamouti scheme when the best antenna is selected.

- For combined CC and STBC systems over independent fading channel, we derive a general upper bound for any N, M and L; a tighter upper bound for the special case of any N, and M when $L = 1$; and another tighter bound for the Alamouti scheme when the best antenna is selected.

- For combined TCM and STBC systems over independent fading channel, we also derive a general upper bound for any N, M and L; a tighter upper bound for the special case of any N, and M when $L = 1$; and exact analysis for the Alamouti scheme when the best antenna is selected.

- For STBC-only systems, and combined CC and STBC systems over space correlated fading channels, general upper bounds are presented for any N, M and L.

Chapter 2

Receive Antenna Selection for Space-Time Block Codes

2.1 Introduction

In this chapter, we present a comprehensive performance analysis of orthogonal space-time block codes (STBCs) with receive antenna selection. We limit our analysis to orthogonal STBCs simply because they are easy to design and they achieve the maximum diversity order possible for a given number of transmit/receive antennas. In our analysis, we assume that, for a given number of receive antennas M, the receiver uses L out of the available M antennas where the selected antennas are those whose instantaneous signal-to-noise ratios are the largest. This is achieved by comparing the sums of the magnitude squares of the fading coefficients at each receive antenna and selecting those (L of them) corresponding to the largest sums. The adopted selection

criterion is clearly optimal in the sense that it maximizes the SNR at the receiver. We acknowledge, however, that the adopted selection criterion does not necessarily result in the best performance, but our interest here is to quantify the impact of antenna selection on the overall diversity order of the system.

We derive two explicit upper bounds on the BER performance for any N, M, and $L \leq M$, where N denotes the number of transmit antennas. The first bound is based on using order statistics, whereas the other bound is based on a simple idea which leads to a relatively tighter bound at low SNR. We show that, with antenna selection, the resulting diversity order is the same as that of the full-complexity system for any number of selected antennas. We also show that the degradation in SNR due to antenna selection is upper bounded by $10\log_{10}(M/L)$ dB. Additionally, we derive a tighter upper bound for the BER performance for any N and M when $L = 1$ and an exact expression for the BER performance for the Alamouti scheme when $L = 1$. We finally present simulation results that support our analysis.

We remark that the problem under consideration is equivalent to receive antenna selection for multiple antenna systems over Nakagami-m fading channels with a single transmit antenna, which has been treated in [41]. Both problems become equivalent when $m = N$. In [41], exact analysis was given for the following cases: any m and M with $L = 1$; and any m, with $M = 3, 4$ and $L = 2$. However, their approach is quite difficult and cannot be extended to the more general case, which is any N , M, and L.

2.2 System Model

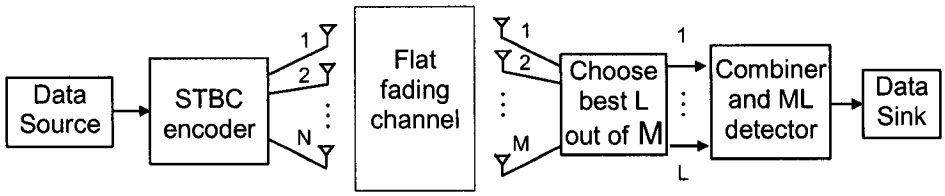

Figure 2.1: System block diagram of STBCs MIMO system.

The system under consideration is shown in Fig. 2.1, which models a wireless communication system that employs N antennas at the transmitter side and M antennas at the receiver side. As shown in the figure, the incoming data is encoded by the STBC encoder according to the encoding mechanism presented in [6]. The outputs of the encoder, which consist of N parallel streams, are then transmitted from the N transmit antennas simultaneously. Blocks that involve modulation, demodulation, etc., have been suppressed from the figure due to their irrelevance in the analysis.

At the receiver, after demodulation, matched-filtering, and sampling, the signal r_t^j received by antenna j at time t is given by

$$r_t^j = \sum_{i=1}^{N} \alpha_{i,j}(t) c_t^i + w_t^j \tag{2.1}$$

where c_t^i is the signal transmitted from antenna i at time t; the noise w_t^j at time t is modeled as independent samples of a zero-mean complex Gaussian random variable with variance $N_0/2$ per dimension. The coefficients $\alpha_{i,j}(t)$ model fading between the i^{th} transmit and j^{th} receive antennas at time t and are assumed to be complex

Gaussian random variables with variance 0.5 per dimension. This is for the channel gain normalization so that the received signal power is the same as the transmitted one. We assume that the fading coefficients are constant over a block of consecutive N symbols and vary independently from one block to another, similar to the channel model adopted in [5] and [6]. This is a necessary assumption to allow for signal decoupling at the receiver. Moreover, the subchannels are assumed to fade independently.

2.3 Performance of Full-Complexity System

Assuming binary phase-shift keying (BPSK) signaling, maximum-likelihood (ML) decoding, and that the channel state information (CSI) is known exactly at the receiver, the conditional BER, conditioned on the channel gains, is expressed as

$$\begin{aligned} P_b(e \mid \boldsymbol{\alpha}) &= Q\left(\sqrt{2\frac{E_s}{N_0}\sum_{i=1}^{N}\sum_{j=1}^{M}|\alpha_{i,j}|^2}\right) \\ &= Q\left(\sqrt{2\frac{E_s}{N_0}\sum_{k=1}^{NM}|\alpha_k|^2}\right) \end{aligned} \tag{2.2}$$

where $\boldsymbol{\alpha} = \{\alpha_{1,1}, \ldots, \alpha_{N,M}\}$, and E_s is the average energy per transmitted symbol. To compute the average bit error rate, we need to average the expression in (2.2) with respect to the random variables $|\alpha_k|^2$ for $k = 1, \ldots, NM$. To simplify the analysis,

we first introduce an auxiliary random variable that we denote Y, defined as

$$Y = \sum_{k=1}^{NM} |\alpha_k|^2 . \tag{2.3}$$

Note that Y is a Chi-square random variable with $2NM$ degrees of freedom with probability density function (pdf) given by [49]

$$f(y) = \frac{1}{(NM-1)!} y^{NM-1} e^{-y}, \quad y \geq 0. \tag{2.4}$$

Consequently, the average BER performance can be shown to be [49]

$$P_b(e) = \left[\frac{1}{2}(1-\mu)\right]^{NM} \sum_{k=0}^{NM-1} \binom{NM-1+k}{k} \cdot \left[\frac{1}{2}(1+\mu)\right]^k \tag{2.5}$$

where

$$\mu \triangleq \sqrt{\frac{\gamma_s}{1+\gamma_s}}.$$

The term $\gamma_s = \frac{E_s}{N_0} E\left(|\alpha_k|^2\right) = \frac{E_s}{N_0}$ represents the average signal-to-noise ratio (SNR) and $E(\cdot)$ is the expectation operator. When the SNR is sufficiently large, the expression is (2.5) can be approximated by [49]

$$P_b(e) \approx \binom{2NM-1}{NM} (4\gamma_s)^{-NM}, \tag{2.6}$$

which clearly shows that the diversity order is NM, which is the maximum achievable diversity order, for a given N transmit and M receive antennas.

2.4 Performance Analysis with Antenna Selection

2.4.1 Upper Bounds on BER for Any N, M, and L

In this section, we derive upper bounds on the BER performance of the system described above for any N, M, and L. Specifically, we derive two bounds using two different approaches. The first approach uses order statistics, whereas the second approach uses a simple idea and results in a relatively tighter bound.

Approach I

Let us define Y_j as

$$Y_j = \sum_{i=1}^{N} |\alpha_{i,j}|^2, \quad j = 1, 2, \ldots, M \tag{2.7}$$

which represents the amount of energy picked up by the j^{th} antenna. Recall that when we select the best L antennas, we observe the sequence $Y_1, Y_2, \ldots, Y_M$ and select those antennas corresponding to the largest L terms of this sequence. To simplify the analysis, we introduce a sequence of M auxiliary random variables, that we denote by $X_1, X_2, \ldots, X_M$, such that

$$X_1 \leq X_2 \leq \cdots \leq X_M.$$

This new sequence is obtained by arranging the random sequence $Y_1, Y_2, \ldots, Y_M$ in a decreasing order of magnitude. Such a sequence may be considered as a random

sample from an absolutely continuous population with pdf [49]

$$f(x) = \frac{1}{(N-1)!} x^{N-1} e^{-x} \tag{2.8}$$

and cumulative distribution function (cdf)

$$F(x) = 1 - \sum_{k=0}^{N-1} \frac{x^k e^{-x}}{k!}, \quad x \geq 0. \tag{2.9}$$

The joint density function of the ordered random variables $X_1, X_2, \ldots, X_M$ can be shown to be [50][1]

$$f_{X_1,\ldots,X_M}(x_1, \ldots, x_M) = \begin{cases} M! \prod_{j=1}^{M} f_{X_j}(x_j), & 0 \leq X_1 \leq X_2 \leq \cdots \leq X_M \\ 0, & \text{otherwise} \end{cases} \tag{2.10}$$

where $f_{X_j}(x_j)$ is given by (2.8). To find the joint density function of $(X_{M-L+1}, \ldots, X_M)$, which we will need later to find the average BER performance, we integrate the joint density function in (2.10) with respect to the variables $(X_1, \ldots, X_{M-L})$ as follows.

[1]It is important to note that the random variables $X_1, X_2, \ldots, X_M$ are no longer independent due to the ordering.

$$
\begin{aligned}
& f_{X_{M-L+1},\cdots,X_M}(x_{M-L+1},\ldots,x_M) \\
&= \int_0^{x_{M-L+1}} \cdots \int_0^{x_2} f_{X_1,\cdots,X_M}(x_1,\ldots,x_M) dx_1 dx_2 \cdots dx_{M-L} \\
&= M! \left(\prod_{j=M-L+1}^{M} f_{X_j}(x_j) \right) \int_0^{x_{M-L+1}} \cdots \int_0^{x_2} \prod_{j=1}^{M-L} f_{X_j}(x_j)\, dx_1 dx_2 \cdots dx_{M-L} \\
&= \frac{M!}{(M-L)!} \left(\prod_{j=M-L+1}^{M} f_{X_j}(x_j) \right) F(x_{M-L+1})^{M-L} \qquad (2.11)
\end{aligned}
$$

When the best L antennas are selected, the conditional probability in (2.2) becomes[2]

$$
\begin{aligned}
P_b(e \mid X_{M-L+1} \leq \cdots \leq X_M) &= Q\left(\sqrt{2\gamma_s \sum_{j=M-L+1}^{M} X_j} \right) \\
&\leq \frac{1}{2} \exp\left(-\gamma_s \sum_{j=M-L+1}^{M} X_j \right), \qquad (2.12)
\end{aligned}
$$

where the last inequality is obtained by applying the Chernoff bound to the first line in (2.12) [49]. To compute the average BER performance, we average the expression in (2.12) with respect to the random variables $(X_{M-L+1},\ldots,X_M)$, whose joint density function is given by (2.11), as follows.

$$
\begin{aligned}
P_b(e) = & \int_0^{\infty} \int_0^{x_M} \cdots \int_0^{x_{M-L+2}} P_b(e \mid X_{M-L+1} \leq \cdots \leq X_M) \\
& \cdot f_{X_{M-L+1},\cdots,X_M}(x_{M-L+1},\ldots,x_M) dx_{M-L+1} \cdots dx_M. \qquad (2.13)
\end{aligned}
$$

[2]When L antennas are selected at a time, there are $\binom{M}{L}$ subsets to choose from, but we assume here that the selected subset is the one that results in the maximum SNR at the receiver.

Obtaining a closed-form expression for the integral in (2.13) is cumbersome and complicated due to the fact that the random variables $X_1, X_2, \ldots, X_M$ are no longer independent. We remark, however, that exact evaluation of a similar expression was done in [41] but only for special cases of M and L. Even for these special cases, the analysis was quite involved. Therefore, to simplify the analysis, we perform the integration over the whole space, resulting in a looser bound. Accordingly (2.13) becomes

$$\begin{aligned} P_b(e) \leq & \int_0^\infty \int_0^\infty \cdots \int_0^\infty P_b(e \mid X_{M-L+1} \leq \cdots \leq X_M) \\ & \cdot f_{X_{M-L+1},\cdots,X_M}(x_{M-L+1}, \ldots, x_M) dx_{M-L+1} \cdots dx_M \\ = & \frac{M!}{2\,(M-L)!} \left[\prod_{k=0}^{L-2} \int_0^\infty e^{-\gamma_s x_{M-k}} f_{X_{M-k}}(x_{M-k}) dx_{M-k} \right] \\ & \cdot \int_0^\infty e^{-\gamma_s x_{M-L+1}} f_{X_{M-L+1}}(x_{M-L+1}) \left(F_{X_{M-L+1}}(x_{M-L+1})\right)^{M-L} dx_{M-L+1}. \end{aligned} \tag{2.14}$$

Note that since the random variables X_j for $j = 1, 2, \ldots, M$ are identical, and so are their distributions, (2.14) may be written in a compact form as

$$P_b(e) \leq \frac{M!}{2\,(M-L)!} I_1^{L-1} I_2 \tag{2.15}$$

where

$$\begin{aligned} I_1 &= \int_0^\infty e^{-\gamma_s x_{M-L+2}} f_{X_{M-L+2}}(x_{M-L+2}) dx_{M-L+2} \\ &= (1+\gamma_s)^{-N}, \end{aligned} \tag{2.16}$$

and

$$I_2 = \int_0^\infty e^{-\gamma_s x_{M-L+1}} f_{X_{M-L+1}}(x_{M-L+1}) \left[F_{X_{M-L+1}}(x_{M-L+1})\right]^{M-L} dx_{M-L+1}. \tag{2.17}$$

It is possible to further simplify the expression in (2.17), but we first need the following result [24].

Lemma 1 *Define*

$$g(v) = 1 - e^{-v} \sum_{k=0}^{N-1} \frac{v^k}{k!}.$$

Then

$$g(v) \leq \frac{v^N}{N!}, \quad \textit{for } v > 0.$$

Proof. Observing that $g(v)$ is the incomplete Gamma function, the proof follows

easily, i.e.,

$$\begin{aligned} g(v) &= \frac{1}{(N-1)!}\int_0^v u^{N-1}e^{-u}du \\ &\leq \frac{1}{(N-1)!}\int_0^v u^{N-1}du \\ &= \frac{v^N}{N!}. \end{aligned}$$

■

With simple mathematical manipulations, we can re-write (2.17) as

$$I_2 = \int_0^\infty e^{-\gamma_s x_{M-L+1}} \frac{1}{(N-1)!} x_{M-L+1}^{N-1} e^{-x_{M-L+1}} \left(1 - \sum_{k=0}^{N-1} \frac{x_{M-L+1}^k e^{-x_{M-L+1}}}{k!}\right)^{M-L} dx_{M-L+1}, \tag{2.18}$$

which can be upper bounded, using the above lemma, as

$$\begin{aligned} I_2 &\leq \int_0^\infty e^{-\gamma_s x_{M-L+1}} \frac{1}{(N-1)!} x_{M-L+1}^{N-1} e^{-x_{M-L+1}} \left(\frac{x_{M-L+1}^N}{N!}\right)^{M-L} dx_{M-L+1} \\ &= \frac{N\left[N\left(M-L+1\right)-1\right]!}{\left(N!\right)^{M-L+1}} \left(1+\gamma_s\right)^{-N(M-L+1)} \end{aligned} \tag{2.19}$$

By substituting the above expressions for I_1 and I_2 into (2.15), we arrive at

$$P_b(e) \leq \frac{M!N\left[N\left(M-L+1\right)-1\right]!}{2\left(M-L\right)!\left(N!\right)^{M-L+1}} \left(1+\gamma_s\right)^{-NM}. \tag{2.20}$$

The expression in (2.20) suggests that the diversity order is maintained with antenna selection for any number of selected antennas. As for the degradation in SNR due

to antenna selection, it is not straightforward to quantify this loss from the above expression. As an alternative, we use another bound that we will derive in the next subsection which shows explicitly that the loss in SNR is upper bounded by $10\log_{10}(M/L)$ dB. In addition, as we will demonstrate later, this bound is relatively loose at low SNR, but becomes tighter at high SNR, especially for low values of L.

Approach II

By knowing that the sum of the largest L out of M nonnegative numbers is always greater than or equal to the average of these M numbers multiplied by L, we have

$$\frac{L}{M}\sum_{i=1}^{N}\sum_{j=1}^{M}|\alpha_{i,j}|^2 \leq \sum_{i=1}^{N}\sum_{j=M-L+1}^{M}|\alpha_{i,j}|^2$$

and consequently the expression in (2.2) can be upper bounded as

$$P_b(e \mid \boldsymbol{\alpha}) \leq Q\left(\sqrt{2\frac{L}{M}\gamma_s\sum_{k=1}^{NM}|\alpha_k|^2}\right). \tag{2.21}$$

By comparing the right-hand side of the expression in (2.21) with that in (2.2), we notice that both are the same except that the SNR in the former expression is scaled by L/M . Therefore, the average BER performance, with antenna selection, will have a similar expression as that in (2.5), namely

$$P_b(e) \leq \left[\frac{1}{2}(1-\mu')\right]^{NM}\sum_{k=0}^{NM-1}\binom{NM-1+k}{k}\cdot\left[\frac{1}{2}(1+\mu')\right]^{k} \tag{2.22}$$

where

$$\mu' \triangleq \sqrt{\frac{\frac{L}{M}\gamma_s}{1+\frac{L}{M}\gamma_s}}.$$

To clearly see the impact of antenna selection on the BER performance, we further approximate the expression in (2.22) by

$$P_b(e) \lesssim \binom{2NM-1}{NM}\left(4\frac{L}{M}\gamma_s\right)^{-NM}. \tag{2.23}$$

By comparing (2.6) and (2.23), it is obvious that the diversity order is maintained with antenna selection as that of the full-complexity system for any $L \leq M$. Moreover, it is now easy to see that the reduction in SNR due to antenna selection is upper bounded by $10\log_{10}(M/L)$ dB. We remark that this bound is tighter than that given by (2.20) for all range of SNR but for larger values of L. Both bounds, however, come within 1 dB from each other at high SNR.

2.4.2 Tighter Upper Bound for Any N and M When $L = 1$

In this subsection, based on the order statistic approach, we derive a tighter upper bound for the BER performance for any N and M when $L = 1$.[3] As such, we define

[3]We acknowledge that this case is similar to a system with one transmit antenna and M receive antennas when $L = 1$ over Nakagami-N fading channels. The latter case was considered in [41] where exact analysis was carried out. However, our approach here is much simpler and, as we will demonstrate later, the resulting upper bound is very close to the exact analysis at medium to high SNR.

Z as

$$Z = X_M \tag{2.24}$$

where, as mentioned above, X_M is the largest term in the sequence $Y_1, Y_2, \ldots, Y_M$. It can be shown that the pdf of Z is given by [50]

$$p_Z(z) = MF(z)^{M-1} f(z), \tag{2.25}$$

where $f(z)$ and $F(z)$ are given by (2.8) and (2.9) respectively.

The conditional BER performance conditioned on Z is then given by

$$P_b(e \mid Z) = Q\left(\sqrt{2\gamma_s Z}\right). \tag{2.26}$$

To compute the average BER performance, we average the expression in (2.26) with respect to the random variable Z as follows.

$$\begin{aligned} P_b(e) &= \int_0^\infty Q\left(\sqrt{2\gamma_s z}\right) p_Z(z) dz \\ &\leq \frac{NM}{(N!)^M} \int_0^\infty Q\left(\sqrt{2\gamma_s z}\right) z^{NM-1} e^{-z} dz \\ &= \frac{(NM)!}{2\,(N!)^M} \left(1 - \sum_{l=0}^{NM-1} \frac{\Gamma\left(l+\frac{1}{2}\right) \gamma_s^{1/2}}{\sqrt{\pi} l!\,(1+\gamma_s)^{l+1/2}}\right) \end{aligned} \tag{2.27}$$

where the above inequality is obtained by applying the result of Lemma 1 to $p_Z(z)$,

i.e.,

$$p_Z(z) \leq \frac{M}{(N!)^{M-1}(N-1)!} z^{NM-1} e^{-z}, \quad z \geq 0.$$

and $\Gamma(x)$ is the gamma function, defined as

$$\Gamma(x) = \int_0^\infty t^{x-1} e^{-t} dt, \quad x > 0. \tag{2.28}$$

Although the above expression does not reveal much information about the resulting diversity order with antenna selection, as we will demonstrate later, this expression yields the tighter BER performance for small values of N and M with $L = 1$.

2.4.3 Exact Analysis for the Alamouti Scheme When $L = 1$

In this subsection, we derive an exact expression for the BER performance for the Alamouti scheme when $L = 1$, i.e., the case $N = 2$, any M, and $L = 1$. When $N = 2$, the expressions in (2.8) and (2.9) become

$$f(x) = xe^{-x}$$

and

$$F(x) = 1 - e^{-x} - xe^{-x}, \quad x \geq 0,$$

respectively. By substituting the above expressions for $f(x)$ and $F(x)$ into (2.25), we arrive at

$$\begin{aligned} p_Z(z) &= MF(z)^{M-1}f(z) \\ &= M\sum_{j=0}^{M-1}\sum_{i=0}^{j} A_{j,i}z^{i+1}e^{-(j+1)z} \end{aligned}$$

where

$$A_{j,i} = (-1)^j \binom{M-1}{j}\binom{j}{i}.$$

By averaging the expression in (2.26) with respect to the random variable Z, we arrive at

$$\begin{aligned} P_b(e) &= \int_0^\infty Q\left(\sqrt{2\gamma_s z}\right) p_Z(z)dz \\ &= M\sum_{j=0}^{M-1}\sum_{i=0}^{j} A_{j,i}\int_0^\infty Q\left(\sqrt{2\gamma_s z}\right) z^{i+1}e^{-(j+1)z}dz. \end{aligned} \tag{2.29}$$

The integrand in the above expression can be evaluated using integration by parts as shown in method 4 of Appendix B, and we have

$$\begin{aligned} &\int_0^\infty Q\left(\sqrt{2\gamma_s z}\right) z^{i+1}e^{-(j+1)z}dz \\ &= \frac{(i+1)!}{2\,(j+1)^{i+2}} - \frac{(i+1)!}{2}\sqrt{\frac{\gamma_s}{\pi}}\sum_{l=0}^{i+1}\frac{\Gamma(l+1/2)}{l!\,(j+1)^{i+2-l}\,(1+j+\gamma_s)^{l+1/2}}. \end{aligned} \tag{2.30}$$

Finally, the average BER performance can be obtained by substituting the expression

given by (2.30) into (2.29). Although the above expression does not reveal much information about the resulting diversity order with antenna selection, as we will demonstrate later, this expression yields the exact BER performance for the cases $N = 2$, any M, and $L = 1$, which is essentially the Alamouti scheme when the receiver uses the best antenna.[4]

2.5 Simulation and Numerical Results

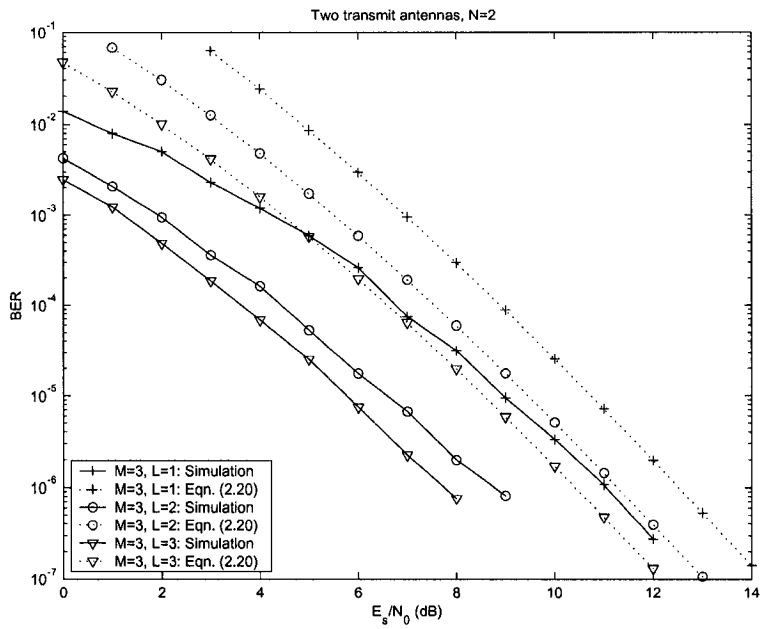

Figure 2.2: BER performance comparison between various antenna selection scenarios for $N = 2$, $M = 3$ along with their upper bounds given by Eqn. (2.20).

In our computer simulations, we used the system model depicted in Fig. 2.1. In

[4]It should be pointed out that Eqn. (2.29) is similar, after proper normalization, to Eqn. (18) in [41] where the latter was derived for a single-transmit, M-receive antenna system when $L = 1$ over Nakagami-N fading channels.

all cases, where applicable, antenna selection is based on maximizing the SNR. In Fig. 2.2, we plot the BER against E_s/N_0 in dB for the cases $N = 2$, $M = 3$, $L = 1, 2, 3$. We also plot on the same figure the upper bounds for these cases given by (2.20). We observe from the figure that all performance curves have the same slope, suggesting that the antenna diversity is maintained with antenna selection. We also observe from the figure that the upper bounds are loose at low SNR, but become tighter at medium to high SNR, especially for small values of L.

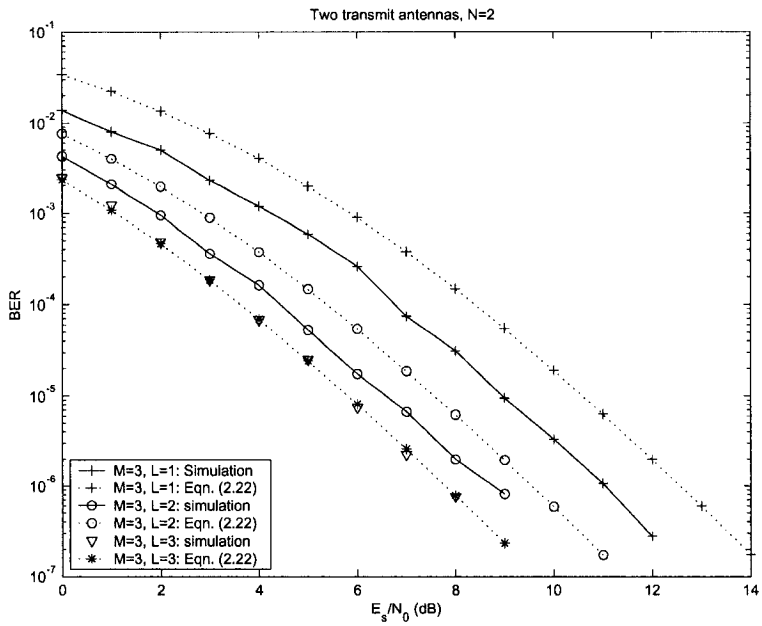

Figure 2.3: BER performance comparison between various antenna selection scenarios for $N = 2$, $M = 3$ along with their upper bounds given by Eqn. (2.22).

In Fig. 2.3, we plot the BER performance for the same cases considered in Fig. 2.2, but here we compare these simulation results against their upper bounds given by (2.22). It is clear from the figure that the diversity order is maintained with antenna

selection. It is also observed from the figure that these upper bounds are tighter for all range of SNR relative to the upper bounds in Fig. 2.2. Moreover, the loss in SNR due to antenna selection for $L = 2$ and $L = 1$ are about 1.0 dB and 3.0 dB at $P_b = 10^{-5}$, respectively, relative to the case $L = 3$. These losses are smaller than their upper bounds (i.e., $10\log_{10}(3/2) = 1.76$ and $10\log_{10}(3) = 4.77$ dB.) We point out here that the gap between this bound and simulations gets smaller as L approaches M. This is simply because the approximation we used to reach at (2.21) becomes more accurate as L increases.

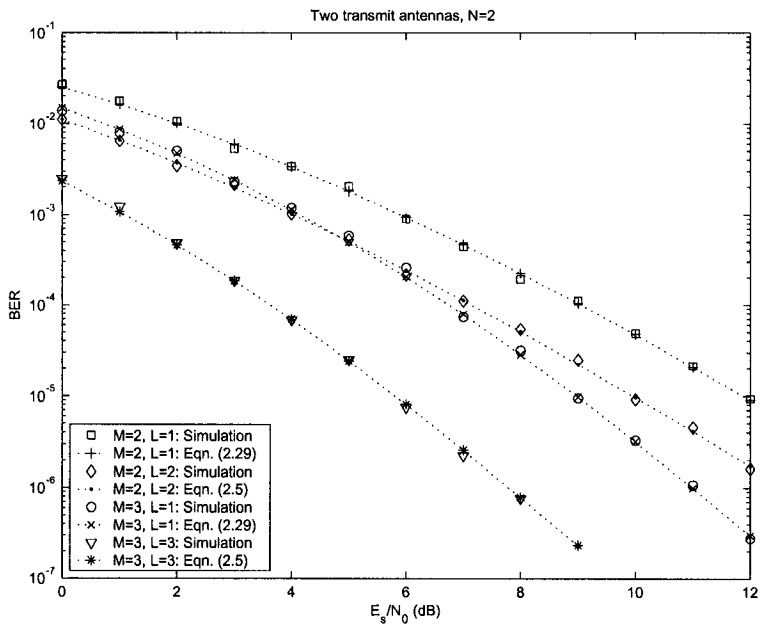

Figure 2.4: BER performance comparison between the full-complexity system and that when the reciever uses the best reveive antenna along with their exact theoretical results given by Eqn. (2.29).

We plot in Fig. 2.4 simulation results along with their theoretical performance based on the expression given by (2.29) for the cases $N = 2$, $M = 2, 3$, and $L = 1, 3$.

It is clear from the figure that the simulation results match perfectly their theoretical results, as expected.

We plot in Fig. 2.5 the BER performance for the case $N = 3$, $M = 2$ and $L = 1$. We also plot on the same figure the corresponding upper bounds given by (2.20), (2.22), and (2.27). It is observed from the figure that all curves have the same slope. More importantly, we observe that the upper bound in (2.27) is very tight and almost overlaps with simulations at high SNR.

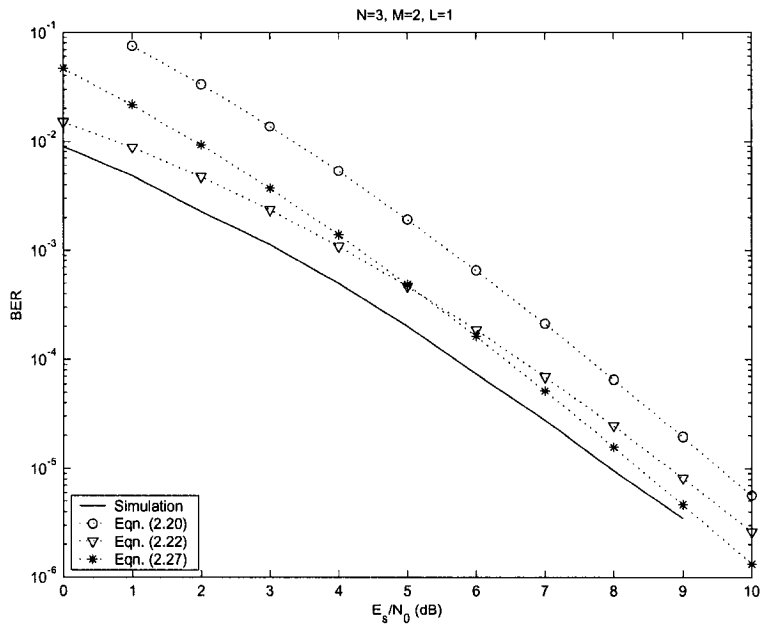

Figure 2.5: BER performance for the case $N = 3$, $M = 2$, and $L = 1$ along with its corresponding upper bounds given by Eqn. (2.20), (2.22), (2.27).

We compare in Fig. 2.6 the asymptotic behavior of the upper bounds given by (2.20) and (2.22) for various cases of antenna selection, particularly, $N = 4$, $M = 4$, and $L = 1, 2, 3$. We also add to the same figure the upper bound in (2.27) for the

case $L = 1$. We observe from the figure that the bound given by (2.20) is quite loose at low SNR, but it falls within 1 dB from that given by (2.22), and it becomes even tighter for the case $L = 1$. This behavior was also observed for other cases of N and M. We attribute this behavior to the fact that the approximation we used to simplify (2.13) (i.e., integrating over the whole space) becomes more accurate as L decreases. It is also clear from the figure that, when $L = 1$, the bound given by (2.27) is the tightest.

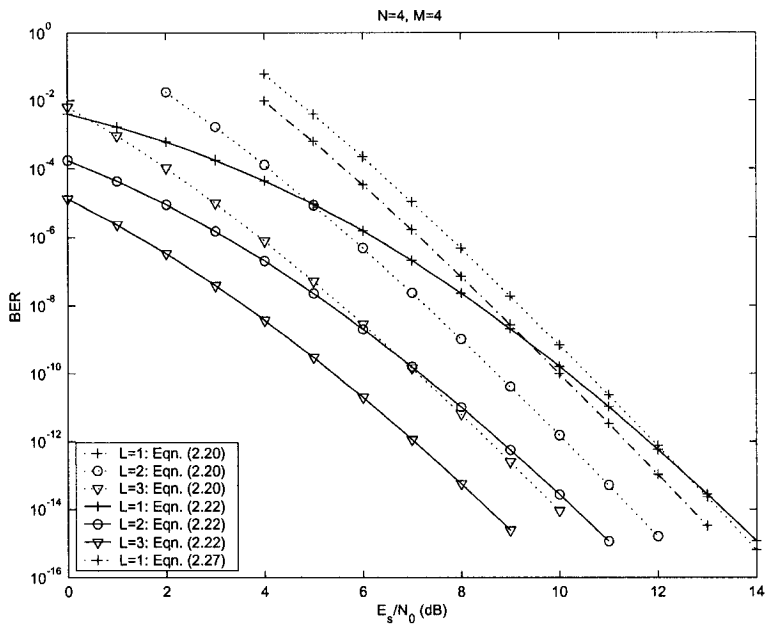

Figure 2.6: A comparison between the asymptotic behavior of the upper bounds given by Eqns. (2.20), (2.22) and (2.27) for various selection scenarios. [Eqn. (2.27) is applicable to the $L = 1$ case only.]

2.6 Conclusions

In this Chapter, we analyzed the performance of orthogonal STBC codes with antenna selection at the receiver. We used a pragmatic selection criterion that maximizes the SNR at the receiver. We derived two explicit upper bounds on the BER performance for any number of transmit and receive antennas and any number of selected antennas. We showed that the diversity order with antenna selection is maintained as that of the full-complexity system, whereas the SNR deteriorates by a value upper bounded by $10\log_{10}(M/L)$ dB. We also derived a tighter upper bound for any N and M when $L = 1$. Furthermore,We derived an expression for the exact BER performance for the Alamouti scheme when $L = 1$. We presented several examples to validate our analysis.

Chapter 3

Receive Antenna Selection for Concatenated Channel Codes and Space-Time Block Codes

3.1 Introduction

In Chapter 2, we consider antenna selection for STBCs only. In this chapter, we present a comprehensive performance analysis of the concatenation scheme that comprises an outer channel code and an inner orthogonal STBC with receive antenna selection. For the outer code, we consider both convolutional code (CC) and trellis-coded modulation (TCM) codes.[1] The latter codes are attractive because they maintain the *full-rate* feature of orthogonal STBCs, unlike the case of CC codes. In

[1]Other types of codes fall under either of these two classes of codes. Thus, their performance analysis follows immediately from the analytical techniques presented in this paper.

particular, we derive upper bounds on the bit error rate (BER) for this concatenation scheme with receive antenna selection. In our analysis, we assume that 1) the receiver uses only L out of the available M receive antennas, where, typically, $L \leq M$, 2) the selected antennas are those that maximize the instantaneous received signal-to-noise ratio (SNR), 3) the channel state information (CSI) is perfectly known at the receiver, and 4) the underlying channel is fully interleaved. We derive an explicit upper bound on the BER for the above concatenation scheme for any N, M and L, where N denotes the number of transmit antennas. We show that the diversity order, with antenna selection, is maintained as that of the full complexity system, whereas the deterioration in SNR is upper bounded by $10\log_{10}(M/L)$ dB. These results are valid for any outer code and any underlying fading channel model. Motivated by the fact that the above upper bound is relatively loose for small values of L, we also derive tighter upper bounds for the following special cases: any N and M when $L = 1$; and $N = 2$, any M when $L = 1$. The former case corresponds to generalized orthogonal STBCs, whereas the latter is essentially the Alamouti scheme when the receiver uses the best antenna. These upper bounds can be extended in a straightforward manner to other types of outer codes and fading channels. Finally, we present simulation results that validate our analysis.

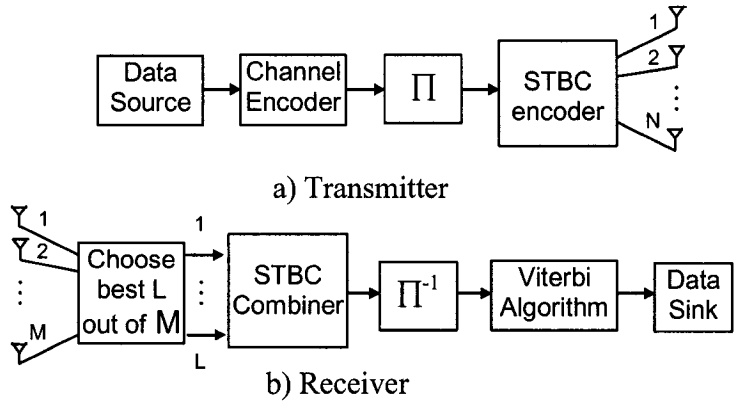

Figure 3.1: System block diagram of concatenated channel codes and STBCs MIMO system.

3.2 System Model

The system under consideration is shown in Fig. 3.1, which models a wireless communication system that employs N transmit and M receive antennas. As shown in the figure, the incoming data is encoded by a channel code of rate r, interleaved, and then encoded by the STBC encoder. The output of the STBC encoder is then transmitted from the N transmit antennas. Blocks that involve modulation, demodulation, etc., have been suppressed from the figure due to their irrelevance in the analysis.

At the receiver, after demodulation, matched-filtering, and sampling, the signal r_t^j received by antenna j at time t is given by

$$r_t^j = \sum_{i=1}^{N} \alpha_{i,j}(t) c_t^i + w_t^j$$

where c_t^i is the signal transmitted from antenna i at time t; the noise w_t^j at time t is

modeled as independent samples of a zero-mean complex Gaussian random variable (rv) with variance $N_0/2$ per dimension. The coefficients $\alpha_{i,j}(t)$ model fading between the i^{th} transmit and j^{th} receive antennas at time instant t and are assumed to be complex Gaussian random variables with variance 0.5 per dimension. In addition, the fading coefficients are assumed to be constant over a block of N consecutive symbols within a frame and vary independently from one block to another. This is a necessary assumption to allow for signal decoupling at the receiver.

3.3 Performance Analysis of the Full-Complexity System

For the purpose of making this chapter self-contained, we review in this section some of the main results, related to our work, on the performance of the above concatenation scheme without antenna selection. We refer to this system as *full-complexity.* When an outer channel code is concatenated with a STBC over fading channels, both time and space diversity gains can be achieved [49]. In such cases, the maximum diversity order that can be achieved is $NMd_{\min}$, where $d_{\min}$ denotes the minimum *Hamming distance* of the outer channel code. For CC codes, $d_{\min}$ is simply the minimum Hamming distance of the code, whereas it represents the minimum symbol-wise Hamming distance for TCM codes. Such diversity gains may be achieved when the underlying STBC is orthogonal and the channel is fully interleaved. The latter condition is normally referred to as *ideal interleaving*, which can be accomplished by using

proper interleaving between the two codes (see Fig. 3.1.) Throughout our analysis, we shall assume that ideal interleaving is achieved, and then later consider more realistic channel models, e.g., block fading.

We remark that the approaches we follow in analyzing the CC and TCM cases are somewhat similar. However, because the resulting upper bounds for one case are not directly applicable to the other, we opt for keeping the analyses of the two cases separate throughout the chapter. We shall start with the CC case.

3.3.1 CC Codes

Let $\mathbf{s}$ and $\mathbf{e}$ denote the transmitted and erroneously decoded codewords, respectively. Also, let $\varphi(\mathbf{s},\mathbf{e})$ denote the set of time indices at which $\mathbf{s}$ and $\mathbf{e}$ differ and $d = |\varphi(\mathbf{s},\mathbf{e})|$ denote the size of $\varphi(\mathbf{s},\mathbf{e})$. Assuming binary phase-shift keying (BPSK), maximum-likelihood (ML) decoding, and that the channel state information (CSI) is perfectly known at the receiver, the conditional pairwise error probability that the receiver will select $\mathbf{e}$ over $\mathbf{s}$ conditioned on the channel gains is given by [35]

$$\begin{aligned} P_2(d \mid \boldsymbol{\alpha}) &= Q\left(\sqrt{2\frac{r}{N}\frac{E_b}{N_0}\sum_{n\in\varphi(\mathbf{s},\mathbf{e})}\sum_{j=1}^{M}\sum_{i=1}^{N}|\alpha_{n,i,j}|^2}\right) \\ &= Q\left(\sqrt{2\frac{r}{N}\frac{E_b}{N_0}\sum_{k=1}^{NMd}|\alpha_k|^2}\right), \end{aligned} \tag{3.1}$$

where $\boldsymbol{\alpha} = \{\alpha_{n,i,j} : n \in \varphi(\mathbf{s},\mathbf{e}),\ i = 1,2,\ldots,N,\ j = 1,2,\ldots,M\}$. To compute the average pairwise error probability, we average the expression in (3.1) with respect

to the probability density function (pdf) of the rvs $|\alpha_k|^2$ for $k = 1, \ldots, NMd$. To simplify the analysis, we first introduce an auxiliary rv that we denote by X, defined as

$$X = \sum_{k=1}^{NMd} |\alpha_k|^2 .$$

Note that X is Chi-square distributed with $2NMd$ degrees of freedom and whose pdf is given as [49]

$$f_X(x) = \frac{1}{(NMd-1)!} x^{NMd-1} e^{-x}, \quad x \geq 0.$$

Consequently, the average pairwise error probability can be shown to be [49]

$$P_2(d) = \left[\frac{1}{2}\left(1 - \sqrt{\frac{\gamma_s}{1+\gamma_s}}\right)\right]^{NMd} \sum_{k=0}^{NMd-1} \binom{NMd-1+k}{k} \left[\frac{1}{2}\left(1 + \sqrt{\frac{\gamma_s}{1+\gamma_s}}\right)\right]^k \tag{3.2}$$

where $\gamma_s = \frac{r}{N}\frac{E_b}{N_0} E[|\alpha_k|^2] = \frac{r}{N}\frac{E_b}{N_0}$ and $E[\cdot]$ is the expectation operator. When the SNR is sufficiently large, the expression in (3.2) can be approximated by [49]

$$P_2(d) \approx \binom{2NMd-1}{NMd} \left(4\frac{r}{N}\frac{E_b}{N_0}\right)^{-NMd}. \tag{3.3}$$

Clearly, at high SNR, the performance is dominated by the minimum Hamming distance of the outer code, which we denote by $d_{\min}$. Consequently, the maximum diversity order is $NMd_{\min}$. The average BER for this scheme is then upper bounded as

[49]

$$P_b \leq \frac{1}{k} \sum_{d=d_{\min}}^{\infty} \beta_d P_2(d), \tag{3.4}$$

where k is the number of bits shifted into the shift register of CC encoder each time, and β_d is the multiplicity corresponding to distance d, and represents the coefficients of the derivative of the CC transfer function.

3.3.2 TCM Codes

Similar to the above case, let $\varphi(\mathbf{s}, \mathbf{e})$ denote the set containing the time indices at which the codewords $\mathbf{s}$ and $\mathbf{e}$ differ and d denote the size of this set. As such, d represents the symbol-wise Hamming distance between $\mathbf{s}$ and $\mathbf{e}$. The conditional pairwise error probability that the receiver will select $\mathbf{e}$ over $\mathbf{s}$ conditioned on the channel gains is given by

$$P_2(d \mid \boldsymbol{\alpha}) = Q\left(\sqrt{\frac{1}{N}\frac{E_s}{2N_0} \sum_{n \in \varphi(\mathbf{s},\mathbf{e})} \sum_{j=1}^{M} \sum_{i=1}^{N} |\alpha_{n,i,j}|^2 \, |s_n - e_n|^2}\right) \tag{3.5}$$

where $|s_n - e_n|^2$ is the normalized squared Euclidean distance between the signal on the correct path and that on the error path at time index n, and E_s/N_0 is the average energy per transmitted symbol. As shown in [51], Chernoff bound of pairwise error probability for TCM will lead to a quite loose BER bound due to the relative low

$d_{\min}$ compared to CC, we use Craig's formula for $Q(x)$ [52]

$$Q(x) = \frac{1}{\pi}\int_0^{\pi/2} \exp(-\frac{x^2}{2\sin^2\theta})d\theta.$$

So, the conditional pairwise error probability given in (3.5) can be represented as

$$\begin{aligned} P_2(d \mid \boldsymbol{\alpha}) &= \frac{1}{\pi}\int_0^{\pi/2} \exp\left(-\frac{1}{N}\frac{E_s}{4N_0}\frac{1}{\sin^2\theta}\sum_{n\in\varphi(\mathbf{s},\mathbf{e})}\sum_{j=1}^{M}\sum_{i=1}^{N}|\alpha_{n,i,j}|^2|s_n-e_n|^2\right)d\theta \\ &= \frac{1}{\pi}\int_0^{\pi/2} \prod_{n\in\varphi(\mathbf{s},\mathbf{e})}\exp\left(-\frac{1}{N}\frac{E_s}{4N_0}\frac{1}{\sin^2\theta}\sum_{j=1}^{M}\sum_{i=1}^{N}|\alpha_{n,i,j}|^2|s_n-e_n|^2\right)d\theta \\ &= \frac{1}{\pi}\int_0^{\pi/2} \prod_{n\in\varphi(\mathbf{s},\mathbf{e})}\exp\left(-\frac{1}{\sin^2\theta}\delta_n^2\sum_{j=1}^{M}\sum_{i=1}^{N}|\alpha_{n,i,j}|^2\right)d\theta \end{aligned} \tag{3.6}$$

where $\delta_n^2 \triangleq \frac{1}{N}\frac{E_s}{4N_0}|s_n - e_n|^2$. Now let us define Y_n as

$$Y_n = \sum_{j=1}^{M}\sum_{i=1}^{N}|\alpha_{n,i,j}|^2, \quad n \in \varphi(\mathbf{s},\mathbf{e}). \tag{3.7}$$

Clearly, the rvs Y_n are independent and Chi-square distributed, each with $2NM$ degrees of freedom and a pdf given by

$$f_Y(y) = \frac{1}{(NM-1)!}y^{(NM-1)}e^{-y}. \tag{3.8}$$

In order to evaluate the average pairwise error probability, we average (3.6) with respect to the distributions of Y_n as

$$\begin{aligned} P_2(d) &= \frac{1}{\pi}\int_0^{\pi/2}\prod_{n\in\varphi(\mathbf{s},\mathbf{e})}\int_0^{\infty}\exp\left(-\frac{1}{\sin^2\theta}\delta_n^2 y_n\right) f_Y(y_n)\, dy_n d\theta \\ &= \frac{1}{\pi}\int_0^{\pi/2}\prod_{n\in\varphi(\mathbf{s},\mathbf{e})}\left(1+\frac{1}{\sin^2\theta}\delta_n^2\right)^{-NM} d\theta \end{aligned} \tag{3.9}$$

At high SNR, (3.9) can be approximated as

$$\begin{aligned} P_2(d) &\approx \frac{1}{\pi}\int_0^{\pi/2}\prod_{n\in\varphi(\mathbf{s},\mathbf{e})}\left(\frac{1}{\sin^2\theta}\delta_n^2\right)^{-NM} d\theta \\ &= \frac{1}{\pi}\int_0^{\pi/2}(\sin\theta)^{2NMd}\, d\theta \prod_{n\in\varphi(\mathbf{s},\mathbf{e})}\left(\delta_n^2\right)^{-NM} \\ &= \binom{2NMd-1}{NMd}\left(\prod_{n\in\varphi(\mathbf{s},\mathbf{e})}\left(|s_n-e_n|^2\right)^{-NM}\right)\left(\frac{1}{N}\frac{E_s}{N_0}\right)^{-NMd}. \end{aligned} \tag{3.10}$$

The last line of (3.10) is obtained by changing the variable $t = ctg\theta$, and then applying the definite integration method 3 in Appendix B. It suggests that the diversity order is $NMd_{\min}$, where $d_{\min}$ is the minimum symbol-wise Hamming distance of the TCM code.[2] An upper bound on the BER can then be found as

$$P_b \le \frac{1}{k\pi}\int_0^{\pi/2}\frac{\partial}{\partial I}\, T\left(\overline{D(\theta)}, I\right)\Big|_{I=1} d\theta \tag{3.11}$$

[2]We point out that the maximum diversity order, i.e., $NMd_{\min}$, is achieved only in the case of ideal interleaving. On the other hand, when the channel is quasi-static fading, the resulting diversity order is NM. Also, for block fading, the diversity order is anywhere between NM and $NMd_{\min}$, depending upon how fast fading is relative to the codeword length. We will elaborate on this later.

where k denotes the number of bits per transmitted symbol, $T(\overline{D(\theta)}, I)$ is the transfer function of the TCM code, which is obtained directly from the corresponding error state diagram [51]. The branch labels of the error state diagram, denoted by $\overline{D(\theta)}$, after being averaged with respect to the fading coefficients, are given by

$$\overline{D(\theta)} = \left(1 + \frac{1}{\sin^2\theta}\delta_n^2\right)^{-NM}. \tag{3.12}$$

The definite integral in (3.11) can be evaluated to any degree of accuracy by numerical integration methods, see [53] and [54]. That is changing the variable $t = cos(2\theta)$, and then applying the numerical integration method 5 in Appendix B.

3.4 Upper Bounds on the BER with Antenna Selection

3.4.1 General Upper Bound for Any N, M and L

In this section, we derive an upper bound on the BER for the above concatenated coding scheme with antenna selection. That is, the case when the receiver uses only L out of the available M receive antennas, where $1 \leq L \leq M$. Note that there are $\binom{M}{L}$ subsets to choose from, but we assume here that the selected subset is the one

that results in the maximum SNR at the receiver. Let us define $W_{n,j}$ as

$$W_{n,j} = \sum_{i=1}^{N} |\alpha_{n,i,j}|^2, \quad n \in \varphi(\mathbf{s}, \mathbf{e}), \; j = 1, 2, \ldots, M, \tag{3.13}$$

which represents the amount of energy picked up by the j^{th} receive antenna at time index n. Without loss of generality, let us assume, at time index n, that we have

$$W_{n,1} \leq W_{n,2} \leq \cdots \leq W_{n,M}, \quad n \in \varphi(\mathbf{s}, \mathbf{e}). \tag{3.14}$$

By knowing that the sum of the largest L out of M nonnegative numbers is always greater than or equal to the average of these M numbers multiplied by L, we have

$$\sum_{j=M-L+1}^{M} \sum_{i=1}^{N} |\alpha_{n,i,j}|^2 \geq \frac{L}{M} \sum_{j=1}^{M} \sum_{i=1}^{N} |\alpha_{n,i,j}|^2. \tag{3.15}$$

Armed with the above simple result, we shall now proceed to derive an upper bound on the BER for both the CC and TCM cases.

CC Codes

When the receiver selects the best L antennas, the conditional pairwise error probability given by (3.1) can be upper bounded as

$$P_2(d \mid \boldsymbol{\alpha}) \leq Q\left(\sqrt{2\frac{r}{N}\frac{L}{M}\frac{E_b}{N_0}\sum_{k=1}^{NMd} |\alpha_k|^2}\right). \tag{3.16}$$

By averaging the the expression in (3.16) with respect to the rvs $|\alpha_k|^2$, we get [49]

$$P_2(d) \leq \left[\frac{1}{2}\left(1-\sqrt{\frac{\frac{L}{M}\gamma_s}{1+\frac{L}{M}\gamma_s}}\right)\right]^{NMd} \sum_{k=0}^{NMd-1} \binom{NMd-1+k}{k} \left[\frac{1}{2}\left(1+\sqrt{\frac{\frac{L}{M}\gamma_s}{1+\frac{L}{M}\gamma_s}}\right)\right]^{k}. \tag{3.17}$$

At high SNR, (3.17) can be approximated as

$$P_2(d) \lesssim \binom{2NMd-1}{NMd} \left(4\frac{r}{N}\frac{L}{M}\frac{E_b}{N_0}\right)^{-NMd}. \tag{3.18}$$

By comparing (3.18) with (3.3), it is obvious that the diversity order is maintained with antenna selection for any $L \leq M$, whereas the SNR is degraded by $10\log_{10}(M/L)$ dB. As for the BER, it can also be upper bounded by using the expression in (3.4) with $P_2(d)$ replaced by its expression in (3.17).

TCM Codes

When the receiver selects the best L antennas, the conditional pairwise error probability given by (3.5) can be upper bounded as

$$\begin{aligned} P_2\left(d \mid \boldsymbol{\alpha}\right) &\leq Q\left(\sqrt{\frac{1}{N}\frac{L}{M}\frac{E_s}{2N_0}\sum_{n\in\varphi(\mathbf{s},\mathbf{e})}\sum_{j=1}^{M}\sum_{i=1}^{N}|\alpha_{n,i,j}|^2\,|s_n-e_n|^2}\right) \\ &= \frac{1}{\pi}\int_0^{\pi/2}\prod_{n\in\varphi(\mathbf{s},\mathbf{e})}\exp\left(-\frac{1}{\sin^2\theta}\frac{L}{M}\delta_n^2\sum_{j=1}^{M}\sum_{i=1}^{N}|\alpha_{n,i,j}|^2\right)d\theta. \end{aligned} \tag{3.19}$$

Averaging (3.19) with respect to the channel gains yields

$$\begin{aligned} P_2(d) &\leq \frac{1}{\pi}\int_0^{\pi/2} \prod_{n\in\varphi(\mathbf{s},\mathbf{e})} \int_0^{\infty} \exp\left(-\frac{1}{\sin^2\theta}\frac{L}{M}\delta_n^2 y_n\right) f_Y(y_n)\, dy_n d\theta \\ &= \frac{1}{\pi}\int_0^{\pi/2} \prod_{n\in\varphi(\mathbf{s},\mathbf{e})} \left(1+\frac{1}{\sin^2\theta}\frac{L}{M}\delta_n^2\right)^{-NM} d\theta \end{aligned} \tag{3.20}$$

where $f_Y(y_n)$ is defined by (3.8). When the SNR is sufficiently large, the expression in (3.20) can be approximated by

$$P_2(d) \lesssim \binom{2NMd-1}{NMd} \left(\prod_{n\in\varphi(\mathbf{s},\mathbf{e})} \left(|s_n - e_n|^2\right)^{-NM}\right) \left(\frac{1}{N}\frac{L}{M}\frac{E_s}{N_0}\right)^{-NMd}. \tag{3.21}$$

which clearly shows that the diversity order is maintained with antenna selection, and the loss in coding gain is upper bounded by $10\log_{10}(M/L)$ dB. An upper bound on the BER can be found by following similar steps that led to (3.11). In this case, the branch labels in (3.12) are replaced with

$$\overline{D(\theta)} = \left(1+\frac{1}{\sin^2\theta}\frac{L}{M}\delta_n^2\right)^{-NM}. \tag{3.22}$$

As we will demonstrate later, the above upper bounds are somewhat loose for small values of L. This motivates us to derive tighter upper bounds for special cases, including generalized orthogonal STBCs and the Alamouti scheme when the receiver selects the best antenna, i.e., $L = 1$.

3.4.2 Tighter Upper Bound for Any N and M When $L = 1$: Bound I

In this section, we take the approach of order statistics to derive an upper bound on the BER for any N and M when $L = 1$. The sequence $W_{n,j}$ for $n \in \varphi(\mathbf{s}, \mathbf{e})$, $j = 1, 2, \ldots, M$, defined by (3.13), may be considered as a random sample from an absolutely continuous population with pdf

$$f(w) = \frac{1}{(N-1)!} w^{N-1} e^{-w}, \quad w \geq 0 \tag{3.23}$$

and cumulative distribution function (cdf)

$$F(w) = 1 - \sum_{k=0}^{N-1} \frac{w^k e^{-w}}{k!}, \quad w \geq 0. \tag{3.24}$$

Let us define Z_n as

$$Z_n = \max\left(W_{n,1}, W_{n,2}, \ldots, W_{n,M}\right). \tag{3.25}$$

The pdf of Z_n is then given by [50]

$$\begin{aligned} p_Z(z) &= MF(z)^{M-1} f(z) \\ &= \frac{M}{(N-1)!} z^{N-1} e^{-z} \left(1 - e^{-z} \sum_{k=0}^{N-1} \frac{z^k}{k!}\right)^{M-1} \end{aligned} \tag{3.26}$$

where $z \geq 0$. Let us also define U as

$$U = \sum_{n=1}^{d} Z_n, \quad n \in \varphi(\mathbf{s}, \mathbf{e}). \tag{3.27}$$

Since the rvs Z_n, for $n \in \varphi(\mathbf{s}, \mathbf{e})$, are independent and identically distributed, the pdf of U may be expressed as

$$p_U(u) = p_Z(u) \circledast p_Z(u) \circledast p_Z(u) \circledast \cdots \circledast p_Z(u), \tag{3.28}$$

where $p_Z(u)$ is defined by (3.26) and $\circledast$ denotes convolution. To find the average pairwise error probability, we will eventually need to do the averaging with respect to $p_U(u)$ as given by (3.28). However, doing so is very difficult because obtaining a closed-form expression for $p_U(u)$ involves convolving n complex terms (see (3.26)), which is cumbersome and complicated to carry out. To simplify the analysis, we first find an approximation of $p_U(u)$ using the following simple result and then use this approximation in the averaging process instead.

Applying the result of the Lemma 1 in Chapter 1 to the right side of (3.26) yields

$$p_Z(z) \leq \frac{M}{(N!)^{M-1}(N-1)!} z^{NM-1} e^{-z}, \quad z \geq 0. \tag{3.29}$$

Let us denote the right side of (3.29) by $h(z)$. As such, $p_U(u)$ can be upper bounded

as

$$\begin{aligned} p_U(u) &= p_Z(u) \circledast p_Z(u) \circledast p_Z(u) \circledast \cdots \circledast p_Z(u) \\ &\leq h(u) \circledast h(u) \circledast h(u) \circledast \cdots \circledast h(u) \\ &= \mathcal{F}^{-1}\left\{\left[\mathcal{F}\left\{h(u)\right\}\right]^d\right\} \\ &= \mathcal{F}^{-1}\left\{\left[\frac{(NM)!}{(N!)^M}\frac{1}{(1+jw)^{NM}}\right]^d\right\} \\ &= \left(\frac{(NM)!}{(N!)^M}\right)^d \frac{1}{\Gamma(NMd)} y^{NMd-1}e^{-y}, \quad y \geq 0, \end{aligned} \tag{3.30}$$

where $\mathcal{F}$ and $\mathcal{F}^{-1}$ denote the Fourier transform and inverse Fourier transform, respectively, and $\Gamma(\cdot)$ is the gamma function, as defined in (2.28) Chapter 2.

CC Codes

When the receiver selects the best antenna, the conditional pairwise error probability (3.1) can be expressed as

$$P_2(d \mid U) = Q\left(\sqrt{2\gamma_s U}\right). \tag{3.31}$$

The average pairwise error probability is then computed by averaging (3.31) with respect to the pdf of U as

$$\begin{aligned} P_2(d) &= \int_0^\infty Q\left(\sqrt{2\gamma_s u}\right) p_U(u) du \\ &\leq \left(\frac{NM}{(N!)^M}\right)^d \frac{1}{\Gamma(NMd)} \int_0^\infty Q\left(\sqrt{2\gamma_s u}\right) u^{NMd-1} e^{-u} du \\ &= \frac{1}{2}\left(\frac{(NM)!}{(N!)^M}\right)^d \left(1 - \sum_{l=0}^{NMld-1} \frac{\Gamma\left(l+\frac{1}{2}\right)\gamma_s^{1/2}}{\sqrt{\pi} l! \left(1+\gamma_s\right)^{l+1/2}}\right) \end{aligned} \tag{3.32}$$

where the above inequality is obtained by substituting the last line of (3.30) for $p_U(u)$ in the above expression. The BER can be upper bounded using (3.4) and the last line of (3.32).

TCM Codes

Let us define $\mathbf{Z}$ as

$$\mathbf{Z} = \{Z_n : \ n \in \varphi(\mathbf{s}, \mathbf{e})\}, \tag{3.33}$$

where Z_n is given by (3.25). When $L = 1$, the conditional pairwise error probability conditioned on $\mathbf{Z}$ can be represented as

$$\begin{aligned} P_2(d \mid \mathbf{Z}) &= Q\left(\sqrt{\frac{1}{N}\frac{E_s}{2N_0}\sum_{n\in\varphi(\mathbf{s},\mathbf{e})} Z_n \left|s_n - e_n\right|^2}\right) \\ &= \frac{1}{\pi}\int_0^{\pi/2} \exp\left(-\frac{1}{N}\frac{E_s}{4N_0}\frac{1}{\sin^2\theta}\sum_{n\in\varphi(\mathbf{s},\mathbf{e})} Z_n \left|s_n - e_n\right|^2\right) d\theta \\ &= \frac{1}{\pi}\int_0^{\pi/2} \prod_{n\in\varphi(\mathbf{s},\mathbf{e})} \exp\left(-\frac{1}{\sin^2\theta}\delta_n^2 Z_n\right) d\theta. \end{aligned} \tag{3.34}$$

Averaging (3.34) with respect to the pdf of $\mathbf{Z}$ yields

$$\begin{aligned} P_2(d\,) &= \frac{1}{\pi}\int_0^{\pi/2} \prod_{n\in\varphi(\mathbf{s},\mathbf{e})} \int_0^{\infty} \exp\left(-\frac{1}{\sin^2\theta}\delta_n^2 z_n\right) p_Z(z_n) dz_n d\theta \\ &\le \frac{1}{\pi}\int_0^{\pi/2} \prod_{n\in\varphi(\mathbf{s},\mathbf{e})} \int_0^{\infty} \exp\left(-\frac{1}{\sin^2\theta}\delta_n^2 z_n\right) h(z_n) dz_n d\theta \\ &= \frac{1}{\pi}\int_0^{\pi/2} \prod_{n\in\varphi(\mathbf{s},\mathbf{e})} \left(\frac{(NM)!}{(N!)^M}\left(1 + \frac{1}{\sin^2\theta}\delta_n^2\right)^{-NM}\right) d\theta. \end{aligned} \tag{3.35}$$

The upper bound in (3.35) can be approximated at high SNR as

$$P_2(d) \lesssim \binom{2NMd-1}{NMd}\left(\prod_{n\in\varphi(\mathbf{s},\mathbf{e})} \left(\left|s_n - e_n\right|^2\right)^{-NM}\right)\left(\frac{(N!)^{1/N}}{((NM)!)^{1/NM}}\frac{1}{N}\frac{E_s}{N_0}\right)^{-NMd}. \tag{3.36}$$

By comparing (3.36) with (3.10), we can easily see that selecting the best receive antenna results in a coding gain loss of $10\log_{10}(\frac{((NM)!)^{1/NM}}{(N!)^{1/N}})$ dB, which is tighter than

the upper bound suggested by (3.21), that is, $10\log_{10}(M/L)$ dB. For instance, when $N = 4$ and $M = 4$, as per (3.36), the loss in coding gain is 4.25 dB, whereas it is 6.0 dB in (3.21). Additionally, an upper bound on the BER can be obtained by following similar steps that we used to arrive at (3.11), where the branch labels of the error state diagram, defined by (3.12), are modified as

$$\overline{D(\theta)} = \frac{(NM)!}{(N!)^M}\left(1 + \frac{1}{\sin^2\theta}\delta_n^2\right)^{-NM}. \tag{3.37}$$

3.4.3 Tighter Upper Bound for the Alamouti Scheme When $L = 1$: Bound II

In this section, we derive a tighter upper bound on the BER for the case when $N = 2$, any M, and $L = 1$, which is essentially the Alamouti scheme when $L = 1$. When $N = 2$, the expressions in (3.23) and (3.24) become

$$f_W(w) = we^{-w}, \quad w \geq 0,$$

and

$$F_W(w) = 1 - e^{-w} - we^{-w}, \quad w \geq 0,$$

respectively. As defined by (3.25), the pdf of Z_n is given by

$$\begin{aligned} f_Z(z) &= MF_W(z)^{M-1} f_W(z) \\ &= M \sum_{j=0}^{M-1} \sum_{i=0}^{j} A_{j,i} z^{i+1} e^{-(j+1)z}, \end{aligned} \tag{3.38}$$

where $A_{j,i} = (-1)^j \binom{M-1}{j} \binom{j}{i}$.

CC Codes

When $L = 1$, the conditional pairwise error probability conditioned on $\mathbf{Z}$ can be represented as

$$\begin{aligned} P_2(d \mid \mathbf{Z}) &= Q\left(\sqrt{2\gamma_s \sum_{n=1}^{d} Z_n}\right) \\ &\leq \frac{1}{2} \exp\left(-\gamma_s \sum_{n=1}^{d} Z_n\right) \\ &= \frac{1}{2} \prod_{n=1}^{d} \exp\left(-\gamma_s Z_n\right), \end{aligned} \tag{3.39}$$

where $\mathbf{Z}$ is defined by (3.25). The average pairwise error probability is then given by

$$P_2(d) = \int_0^\infty \cdots \int_0^\infty Q\left(\sqrt{2\gamma_s \sum_{n=1}^{d} z_n}\right) f_Z(z_1) \cdots f_Z(z_d) dz_1 \cdots dz_d. \tag{3.40}$$

Substituting (3.38) and (3.39) into (3.40) yields

$$\begin{aligned} P_2(d\,) &\leq \frac{1}{2}\left(\int_0^{\infty} \exp\left(-\gamma_s z\right)\cdot f_Z(z)dz\right)^d \\ &= \frac{1}{2}\left(M\sum_{j=0}^{M-1}\sum_{i=0}^{j} A_{j,i}\frac{(i+1)!}{(j+1+\gamma_s)^{i+2}}\right)^d. \end{aligned} \tag{3.41}$$

It is not possible to simplify this expression further in order to obtain a tighter upper bound on the loss in coding gain due to antenna selection. Nevertheless, as we will demonstrate later, this new upper bound is very tight at all SNR. As for the BER, it can be upper bounded by using the expressions in (3.4) and (3.41).

TCM Codes

When $L = 1$, averaging (3.34) over $\mathbf{Z}$ with pdf $f_Z(z_n)$ given by (3.38) yields

$$\begin{aligned} P_2(d\,) &= \frac{1}{\pi}\int_0^{\pi/2}\prod_{n\in\varphi(\mathbf{s},\mathbf{e})}\int_0^{\infty}\exp\left(-\frac{1}{\sin^2\theta}\delta_n^2 z_n\right) f_Z(z_n)dz_n d\theta \\ &= \frac{1}{\pi}\int_0^{\pi/2}\prod_{n\in\varphi(\mathbf{s},\mathbf{e})}\left(M\sum_{j=0}^{M-1}\sum_{i=0}^{j} A_{j,i}\,(i+1)!\left(1+j+\frac{1}{\sin^2\theta}\delta_n^2\right)^{-(i+2)}\right)d\theta. \end{aligned} \tag{3.42}$$

As for the BER, we upper bound it using (3.11), with $\overline{D\,(\theta)}$ replaced by

$$\overline{D(\theta)} = \left(M\sum_{j=0}^{M-1}\sum_{i=0}^{j} A_{j,i}\,(i+1)!\left(1+j+\frac{1}{\sin^2\theta}\delta_n^2\right)^{-(i+2)}\right). \tag{3.43}$$

As we will demonstrate later, the expression in (3.42) yields *exact* analytical results, where it can be easily evaluated using numerical techniques.

3.5 Simulation and Numerical Results

In our simulations, we use the system model depicted in Fig. 3.1. In all cases, it is assumed, unless otherwise stated, that the channel fading coefficients remain fixed over a block of N consecutive symbols and change independently from one block to another. It is also assumed, where applicable, that antenna selection is based on maximizing the SNR. For the CC code, we use a rate 1/2 code with generator polynomials $(7,5)_{oct}$, and use BPSK modulation. The minimum distance for this code is $d_{\min} = 5$. Since the underlying STBCs are orthogonal, the maximum diversity order is $5NM$. For the TCM code, we use a rate 2/3, 4-state, 8−PSK TCM scheme presented in [55]. The effective length for this code is $d_{\min} = 2$. Consequently, the maximum diversity order is $2NM$. More detailed elaboration on these two codes, e.g., transfer function can be found in Appendix A.2 and A.3.

3.5.1 Interleaver Effect on Performance

Throughout our analysis above, we assume that the underlying channel is fully interleaved. However, in our simulation model, we assume that the fading coefficients remain constant over a block of at least N consecutive symbols in a frame. (We denote the length of this block by L'.) Clearly, to achieve ideal interleaving (or at

least get close to it), one must use interleaving between the outer channel code and the orthogonal STBC. However, the effectiveness of interleaving greatly depends on the value of L' relative to the codeword length, denoted by N'. In this subsection, we investigate the effect of interleaving on the achievable diversity order.

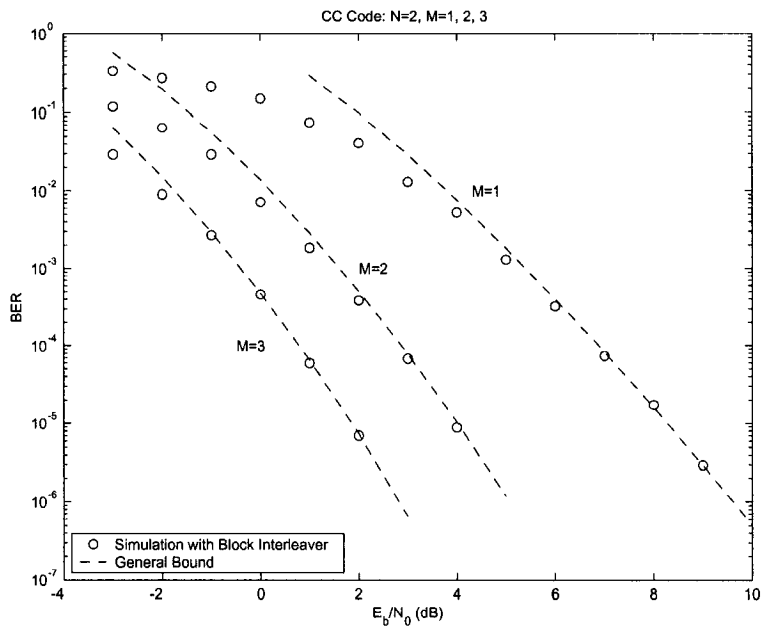

Figure 3.2: BER performance comparison of the full-complexity system with block interleaving (CC case).

In Fig. 3.2, we plot the BER performance against E_b/N_0 in dB for the cases $N = 2$, $M = 1, 2, 3$ when the receiver uses all available antennas with block interleaving (for the CC case). By block interleaving, we mean that the employed interleaver swaps the odd indexed convolutional coded symbols between two consecutive convolutional frames before they are fed into the STBC encoder. Thus, independent fading is guaranteed among coded symbols within a frame. On the same figure, we plot the

performance bounds for these cases using (3.2) and (3.4) (only the first 5 terms in the sum are considered). It is clear from the figure that, the maximum diversity order, which is $10M$, is achieved. We also observe the bound is loose for BER ranging from 10^{-1} to 10^{-3}. This is because the union bound does not account for the intersection of the pairwise decision region.

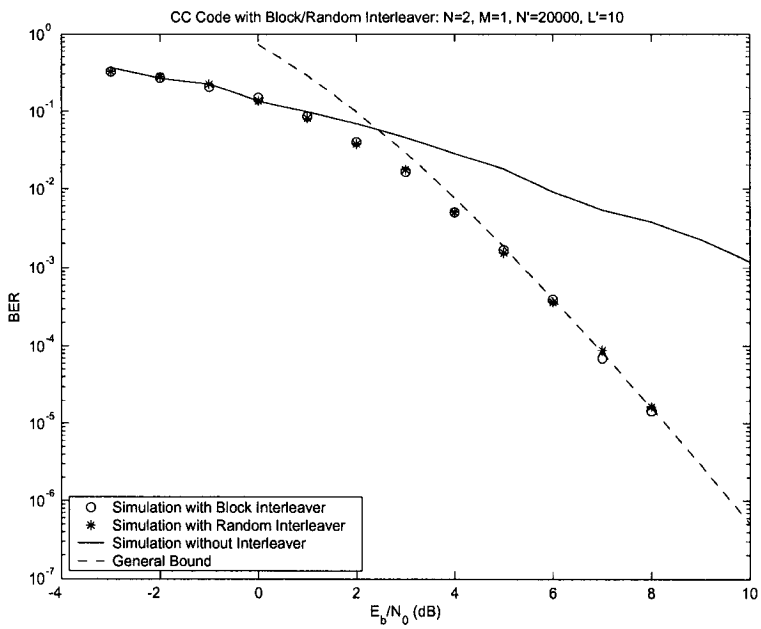

Figure 3.3: BER performance comparison of the full-complexity system with and without interleaving (CC case).

We also examine the performance of the above concatenation system when there is no interleaving and compare it with the case of block interleaving. In our simulations, we assume a block of length $L' = 10$ within a frame of length $N' = 20000$. The simulation results are plotted in Fig. 3.3 (for the CC case). On the same figure, we also plot the simulation results for the case when the block interleaver is replaced

with a pseudo-random interleaver. We observe from the figure that both random and block interleaving achieve the maximum diversity order, whereas much of the available diversity is lost in the absence of interleaving. We attribute this to the fact that $L' \ll N'$, which makes interleaving effective. Though, we expect the achievable diversity order to deteriorate as L' increases with a fixed N', and the diversity order becomes exactly NM when $L' = N'$. Similar results were observed for the TCM case. For the rest of the simulations, we assume that $L' = N$, and therefore the maximum diversity order can be easily achieved with block or pseudo-random interleaving.

3.5.2 General Upper Bound

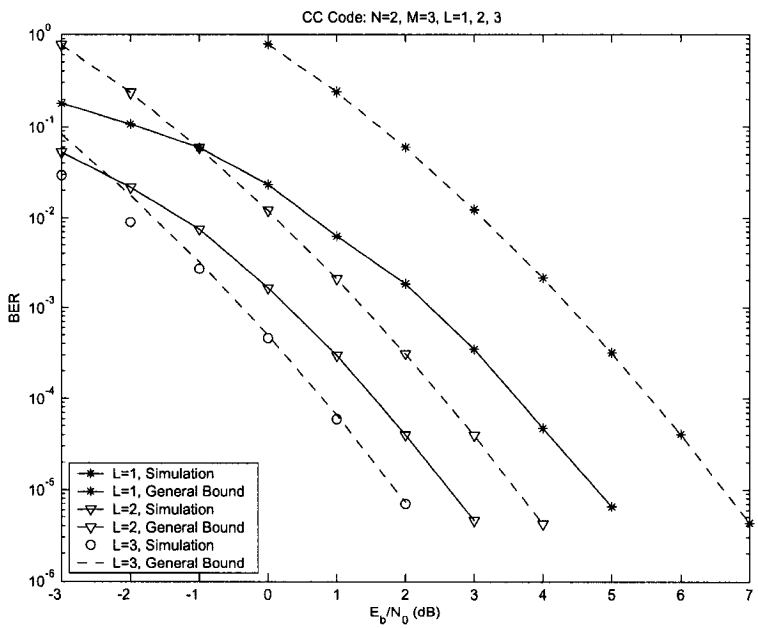

Figure 3.4: BER performance comparison between various antenna selection scenarios along with their upper bounds (CC case).

In Fig. 3.4, we plot the BER performance for the cases $N = 2, M = 3, L = 1, 2, 3$ along with their general upper bounds derived above (for the CC case). It is clear from the figure that all curves have the same slope, suggesting that they have the same diversity order as that of the full complexity system, which agrees with our analytical results derived above. Moreover, the loss in SNR due to antenna selection for $L = 2$ and $L = 1$ are about 0.8 dB and 3.0 dB at $P_b = 10^{-5}$, respectively, relative to the case $L = 3$ (i.e., no selection.) These losses are smaller than their upper bounds (i.e., $10\log_{10}(3/2) = 1.76$ and $10\log_{10}(3) = 4.77$ dB.) We also observe from the figure that the gap between the simulations and their upper bounds gets smaller as L approaches M. This is simply because the approximation we used to arrive at (3.15) becomes more accurate as L increases.

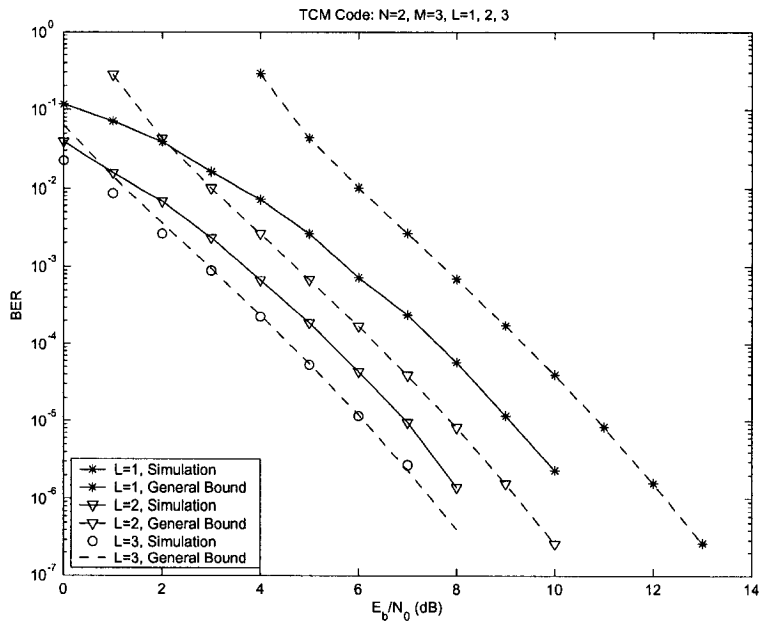

Figure 3.5: BER performance comparison between various antenna selection scenarios along with their upper bounds (TCM case).

We repeat the above experiment for the TCM case. The simulation results along with their respective general upper bounds are plotted in Fig. 3.5. It is clear from the figure that all curves have the same slope, which, again, suggests that the diversity order is maintained with antenna selection. Moreover, the loss in SNR due to antenna selection for $L = 2$ and $L = 1$ are about 0.8 dB and 3.0 dB at $P_b = 10^{-5}$, respectively, relative to the case $L = 3$ (i.e., no selection.)

3.5.3 Tighter Upper Bounds

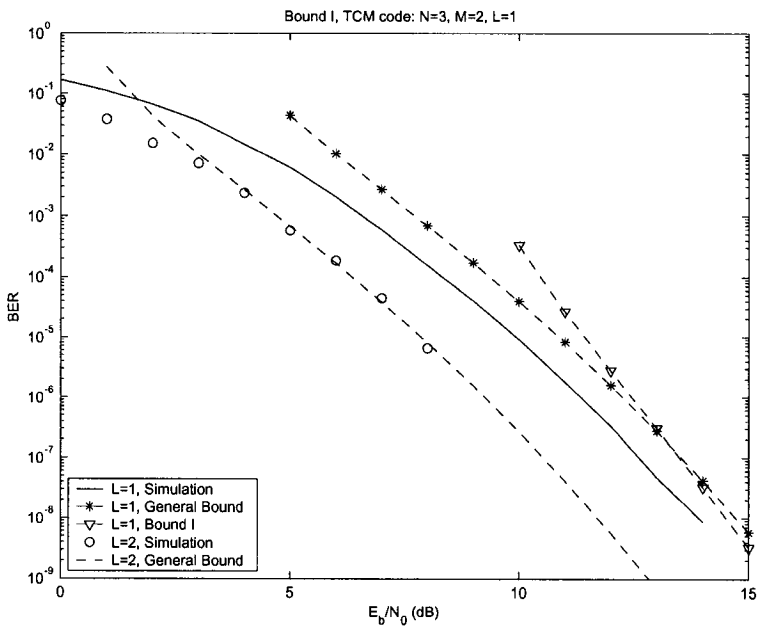

Figure 3.6: BER performance comparison between simulations, general upper bound, and *Bound I* for the cases $N = 3, M = 2, L = 1, 2$ (TCM case).

We plot in Fig. 3.6 the BER performance for the cases $N = 3, M = 2, L = 1, 2$ (for the TCM case.) We also plot on the same figure the corresponding general upper

bound and tighter upper bound (*Bound I*) derived above.We observe from the figure that all curves have the same slope. More importantly, we observe that *Bound I* is looser at low SNR but becomes tighter at high SNR.

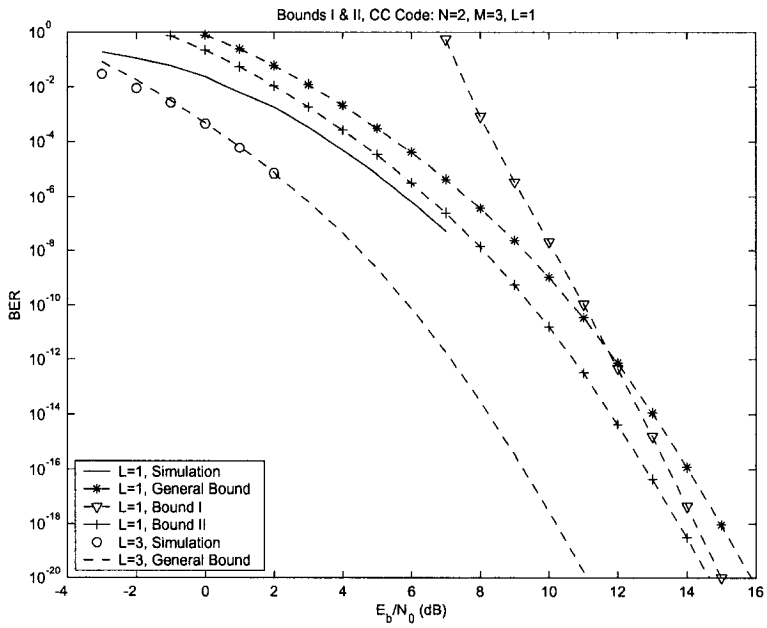

Figure 3.7: BER performance comparison among the general bound, *Bounds I* and *II* for the cases $N = 2, M = 3, L = 1, 3$ (CC case).

In Fig. 3.7, we compare the three bounds for the CC code for the case $N = 2, M = 3, L = 1, 3$, along with the corresponding simulation results. We observe from the figure that *Bound II* is the tightest at all SNR but *Bound I* catches up with it at high SNR.

In Fig. 3.8, we plot the BER performance along with the corresponding *Bound II* for the TCM scheme for the cases $N = 2, M = 3, L = 1, 3$. We observe from the figure the perfect match between the simulation results and their theoretical results.

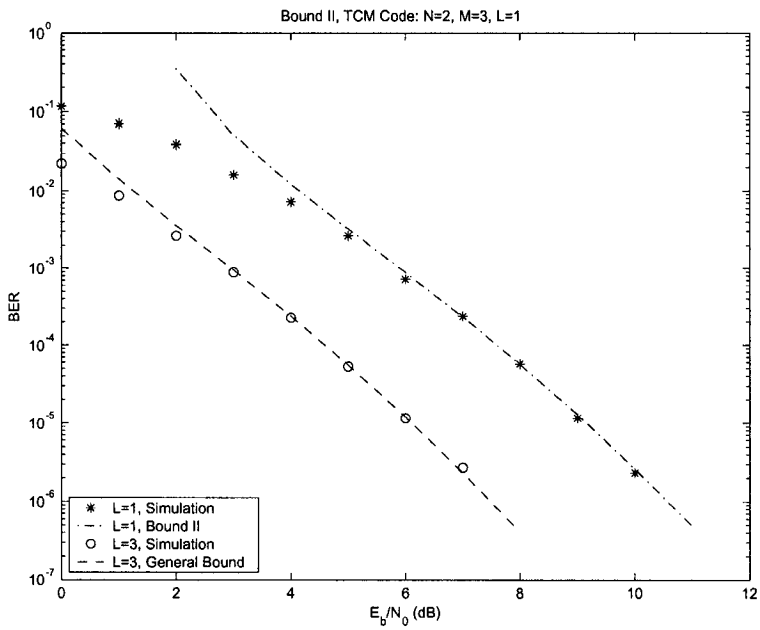

Figure 3.8: BER performance comparison between simulations and *Bound II* for the cases $N = 2, M = 3, L = 1, 3$ (TCM case).

3.6 Conclusions

In this chapter, we analyzed the performance of combined channel coding and space-time block coding with receive antenna selection. We derived upper bounds on the BER performance of this concatenation scheme, including two tighter bounds when the receiver uses the best antenna. We showed that the diversity order with antenna selection is maintained as that of the full-complexity system, whereas the coding gain deteriorates by a value upper bounded by $10\log_{10}(M/L)$ dB. These results can be extended in a straightforward manner to other types of codes, as well as other types of fading. We also presented several examples through which we validated our analytical results.

Chapter 4

Receive Antenna Selection for Space-Time Block Codes Over Correlated Rayleigh Fading Channels

4.1 Introduction

This chapter studies the performance of combined convolutional coding and orthogonal space-time block coding with receive antenna selection over correlated Rayleigh fading channels. In particular, we derive upper bounds on the bit error rate (BER) for the above concatenation scheme with antenna selection. In our analysis, we consider transmit correlation, receive correlation, or joint transmit-receive correlation.

We also assume that the receiver uses only L out of the available M receive antennas, where, typically, $L \leq M$. The selected antennas are those that maximize the instantaneous received signal-to-noise ratio (SNR). Our analytical bounds show that the diversity order, with antenna selection, is the same as that of the full complexity system, whereas the deterioration in SNR is upper bounded by $10\log_{10}(M/L)$ dB. We also quantify the loss in coding gain due to the presence of spatial correlation. This result holds for any N, M and L, where N denotes the number of transmit antennas. We also present several numerical examples that validate our analysis.

4.2 System Model

The systems under consideration in this chapter are the same as those considered in Chapters 2 and 3 except that the subchannel fading coefficients are no longer independent. A widely accepted model for the correlated Raylaigh fading channel is given by

$$\mathbf{H} = \mathbf{R}_t^{1/2}\mathbf{G}\mathbf{R}_r^{1/2} \tag{4.1}$$

where $\mathbf{H}$ represents the $M \times N$ MIMO channel matrix with entries $\alpha_{j,i}$, $i = 1, 2, \ldots, N$, $j = 1, 2, \ldots, M$. The entries $\alpha_{j,i}$ model fading between the i^{th} transmit and j^{th} receive antennas. $\mathbf{R}_t = E\left[\mathbf{H}^H\mathbf{H}\right]$ is the $N \times N$ transmit correlation matrix, and $\mathbf{R}_r = E\left[\mathbf{H}\mathbf{H}^H\right]$ is the $M \times M$ receive correlation matrix. The superscript $\mathbf{H}$ denotes Hermitian transpose, and $E[\cdot]$ denotes expectation. $\mathbf{G}$ is the $M \times N$ i.i.d. complex

Gaussian matrix with zero mean and unit variance entries.

This model incorporates three assumptions as explained explicitly in [44], 1) the correlation between the fading from two transmit antennas to the same receive antenna is transmit correlation and does not depend on the receive antenna; 2) the correlation between the fading from a transmit antenna to two different receive antennas is receive correlation and does not depend on the transmit antenna; 3) the correlation between the fading of two distinct antenna pairs is the product of the corresponding transmit correlation and receive correlation. So, we have the correlation matrix of the vectorized channel $\mathbf{R} = vec(\mathbf{H})vec(\mathbf{H})^H = \mathbf{R}_t \otimes \mathbf{R}_r$ [47], where $vec(\cdot)$ denotes vectorization operation and $\otimes$ denotes Kronecker product. In the case $\mathbf{R}_r = \mathbf{I}_M$, and $\mathbf{R}_t = \mathbf{I}_N$, the model simplifies to the ideally uncorrelated MIMO channel. If $\mathbf{R}_r = \mathbf{I}_M$, and $\mathbf{R}_t \neq \mathbf{I}_N$, the model represents transmit correlation only. That is, the receive antennas are assumed to be placed in a rich scattering environment, whereas there are not many scatterers around the transmit antennas, which is typical in the downlink channel in mobile communication systems. On the other hand, the case $\mathbf{R}_r \neq \mathbf{I}_M$, and $\mathbf{R}_t = \mathbf{I}_N$ represents the receive correlation only scenario. The joint transmit-receive correlation represents the scenario when both the transmit and receive correlation exist. That is when $\mathbf{R}_r \neq \mathbf{I}_M$, and $\mathbf{R}_t \neq \mathbf{I}_N$.

4.3 Performance Analysis of the Full-Complexity System over Correlated Channels

We review in this section the performance of the above coding scheme without antenna selection. We refer to this system as *full-complexity*. First, we consider orthogonal STBC-only system. Then we extend the analysis to the combined CC and STBC scheme. We remark that the approaches we follow in analyzing these two systems are somewhat similar. However, in order to show the antenna diversity contributed by the MIMO channel and time diversity introduced by CC, we opt for keeping the analyses of the two systems separate throughout the chapter. We shall start with the STBC-only case. We assume in our analysis binary phase-shift keying (BPSK) signaling, maximum-likelihood (ML) decoding, and that the channel state information (CSI) is known exactly at the receiver.

4.3.1 Orthogonal STBC-Only System

The conditional BER, conditioned on the channel gains, can be expressed as

$$P_b(e \mid \boldsymbol{\alpha}) = Q\left(\sqrt{2\frac{E_s}{N_0}\sum_{j=1}^{M}\sum_{i=1}^{N}|\alpha_{j,i}|^2}\right) \tag{4.2}$$

where, E_s is the average energy per symbol per each transmit antenna. By using Craig's formula for $Q(x)$ [52], we have

$$P_b(e \mid \boldsymbol{\alpha}) = \frac{1}{\pi} \int_0^{\pi/2} \exp\left(-\frac{E_s}{N_0} \frac{1}{\sin^2\theta} \sum_{j=1}^{M} \sum_{i=1}^{N} |\alpha_{j,i}|^2 \right) d\theta.$$

Denoting $E[\cdot]$ as the expectation operation with respect to channel coefficients $\boldsymbol{\alpha} = \{\alpha_{j,i} : \ j = 1, 2, \ldots, M, \ i = 1, 2, \ldots, N\}$, the average BER can be expressed as

$$P_b(e) = \frac{1}{\pi} \int_0^{\pi/2} E\left[\exp\left(-\frac{E_s}{N_0} \frac{1}{\sin^2\theta} \sum_{j=1}^{M} \sum_{i=1}^{N} |\alpha_{j,i}|^2 \right) \right] d\theta.$$

It can be expressed in the form of the correlation matrix of the vectorized channel by using the characteristic function of quadratic form of complex normal variable [56],

$$\begin{aligned} P_b(e) &= \frac{1}{\pi} \int_0^{\pi/2} \left[\det\left(\mathbf{I}_{MN} + \frac{E_s}{N_0} \frac{1}{\sin^2\theta} \mathbf{R} \right) \right]^{-1} d\theta \\ &= \frac{1}{\pi} \int_0^{\pi/2} \prod_{k=1}^{r(\mathbf{R})} \left[1 + \frac{E_s}{N_0} \frac{1}{\sin^2\theta} \lambda_k(\mathbf{R}) \right]^{-1} d\theta \end{aligned} \tag{4.3}$$

where $r(\mathbf{X})$ denotes the rank of matrix $\mathbf{X}$, and $\lambda_k(\mathbf{X})$, $k = 1, 2, \cdots, r(\mathbf{X})$ are the eigenvalues of $\mathbf{X}$.

Let $\mathbf{R}_t = \mathbf{U}\Lambda_t\mathbf{U}^H$, and $\mathbf{R}_r = \mathbf{V}\Lambda_r\mathbf{V}^H$, where $\mathbf{U}$ and $\mathbf{V}$ are unitary, and Λ_t and Λ_r are diagonal. By using the following property of Kronecker products $(\mathbf{A} \otimes \mathbf{B})(\mathbf{F} \otimes \mathbf{G})$

$= (\mathbf{AF}) \otimes (\mathbf{BG})$, we have

$$\mathbf{R} = \mathbf{R}_t \otimes \mathbf{R}_r = (\mathbf{U} \otimes \mathbf{V}) (\Lambda_t \otimes \Lambda_r) \left(\mathbf{U}^H \otimes \mathbf{V}^H\right). \tag{4.4}$$

Since $\mathbf{U}$ and $\mathbf{V}$ are unitary, it follows that $(\mathbf{U} \otimes \mathbf{V})$ is unitary as well. Hence (4.4) is an eigenvalue decomposition of $\mathbf{R}$ and the diagonal matrix $(\Lambda_t \otimes \Lambda_r)$ contains the eigenvalues of $\mathbf{R}$. So the expression in (4.3) can be represented as

$$P_b(e) = \frac{1}{\pi} \int_0^{\pi/2} \prod_{i=1}^{r(\mathbf{R}_t)} \prod_{j=1}^{r(\mathbf{R}_r)} \left[1 + \frac{E_s}{N_0} \frac{1}{\sin^2\theta} \lambda_i(\mathbf{R}_t) \lambda_j(\mathbf{R}_r)\right]^{-1} d\theta. \tag{4.5}$$

At high SNR, (4.5) can be approximated as

$$\begin{aligned} P_b(e) \approx & \binom{2r(\mathbf{R}_t)r(\mathbf{R}_r) - 1}{r(\mathbf{R}_t)r(\mathbf{R}_r)} \left\{ \left[\prod_{i=1}^{r(\mathbf{R}_t)} \lambda_i(\mathbf{R}_t)\right]^{\frac{1}{r(\mathbf{R}_t)}} \right. \\ & \left. \cdot \left[\prod_{j=1}^{r(\mathbf{R}_r)} \lambda_j(\mathbf{R}_r)\right]^{\frac{1}{r(\mathbf{R}_r)}} \left(4\frac{E_s}{N_0}\right) \right\}^{-r(\mathbf{R}_t)r(\mathbf{R}_r)}. \end{aligned} \tag{4.6}$$

This suggests that the diversity order in the case of joint transmit-receive correlation is $r(\mathbf{R}_t)r(\mathbf{R}_r)$. Clearly if the matrices $\mathbf{R}_t$ and $\mathbf{R}_r$ are full rank, then the diversity order in this case will be NM, which is the diversity order achieved with independent fading. However, the penalty due to correlation is a loss in coding gain. In contrast, when there is no correlation, (4.6) simplifies to

$$P_b(e) \approx \binom{2NM - 1}{NM} \left(4\frac{E_s}{N_0}\right)^{-NM}. \tag{4.7}$$

By comparing (4.6) and (4.7), we can see that the loss in coding gain due to the presence of correlation is given by

$$10\log_{10}\left(\left[\prod_{i=1}^{r(\mathbf{R}_t)}\lambda_i\left(\mathbf{R}_t\right)\right]^{-\frac{1}{r(\mathbf{R}_t)}}\left[\prod_{j=1}^{r(\mathbf{R}_r)}\lambda_j\left(\mathbf{R}_r\right)\right]^{-\frac{1}{r(\mathbf{R}_r)}}\right)\text{dB}. \tag{4.8}$$

4.3.2 Combined CC and Orthogonal STBC System

Let $\mathbf{s}$ and $\mathbf{e}$ denote the transmitted and erroneously decoded codewords, respectively. Also, let $\varphi(\mathbf{s},\mathbf{e})$ denote the set of time indices at which $\mathbf{s}$ and $\mathbf{e}$ differ and $d=|\varphi(\mathbf{s},\mathbf{e})|$ denote the size of $\varphi(\mathbf{s},\mathbf{e})$. The conditional pairwise error probability that the receiver will select $\mathbf{e}$ over $\mathbf{s}$ conditioned on the channel gains is given by

$$\begin{aligned} P_2(d\mid\boldsymbol{\alpha}) &= Q\left(\sqrt{2\frac{r}{N}\frac{E_b}{N_0}\sum_{n=1}^{d}\sum_{j=1}^{M}\sum_{i=1}^{N}|\alpha_{n,i,j}|^2}\right) \\ &= \frac{1}{\pi}\int_0^{\pi/2}\exp\left(-\frac{r}{N}\frac{E_b}{N_0}\frac{1}{\sin^2\theta}\sum_{n=1}^{d}\sum_{j=1}^{M}\sum_{i=1}^{N}|\alpha_{n,j,i}|^2\right)d\theta, \end{aligned} \tag{4.9}$$

where $\boldsymbol{\alpha}=\{\alpha_{n,i,j}: n\in\varphi(\mathbf{s},\mathbf{e}),\ i=1,2,\ldots,N,\ j=1,2,\ldots,M\}$ and E_b denotes the average bit energy.

To compute the average pairwise error probability, we average the expression in (4.9) with respect to $\boldsymbol{\alpha}$.

$$P_2(d)=\frac{1}{\pi}\int_0^{\pi/2}E\left[\exp\left(-\frac{r}{N}\frac{E_b}{N_0}\frac{1}{\sin^2\theta}\sum_{n=1}^{d}\sum_{j=1}^{M}\sum_{i=1}^{N}|\alpha_{n,j,i}|^2\right)\right]d\theta$$

With ideal interleaving, the fading coefficients experienced by each symbol within a codeword are independent, and thus the average pairwise error probability can be represented as

$$\begin{aligned} P_2(d) &= \frac{1}{\pi}\int_0^{\pi/2}\left\{E\left[\exp\left(-\frac{r}{N}\frac{E_b}{N_0}\frac{1}{\sin^2\theta}\sum_{j=1}^{M}\sum_{i=1}^{N}|\alpha_{1,j,i}|^2\right)\right]\right\}^d d\theta \\ &= \frac{1}{\pi}\int_0^{\pi/2}\left[\det\left(\mathbf{I}_{MN}+\frac{r}{N}\frac{E_b}{N_0}\frac{1}{\sin^2\theta}\mathbf{R}\right)\right]^{-d} d\theta \\ &= \frac{1}{\pi}\int_0^{\pi/2}\prod_{i=1}^{r(\mathbf{R}_t)}\prod_{j=1}^{r(\mathbf{R}_r)}\left[1+\frac{r}{N}\frac{E_b}{N_0}\frac{1}{\sin^2\theta}\lambda_i(\mathbf{R}_t)\lambda_j(\mathbf{R}_r)\right]^{-d} d\theta. \end{aligned} \tag{4.10}$$

The average BER for this scheme is then upper bounded as

$$P_b \leq \sum_{d=d_{\min}}^{\infty}\beta_d P_2(d) \tag{4.11}$$

where β_d is the multiplicity of CC corresponding to distance d.

At high SNR, (4.10) can be approximated as

$$\begin{aligned} P_2(d) \approx \binom{2r(\mathbf{R}_t)r(\mathbf{R}_r)d-1}{r(\mathbf{R}_t)r(\mathbf{R}_r)d} &\left\{\left[\prod_{i=1}^{r(\mathbf{R}_t)}\lambda_i(\mathbf{R}_t)\right]^{\frac{1}{r(\mathbf{R}_t)}}\right. \\ &\left.\cdot\left[\prod_{j=1}^{r(\mathbf{R}_r)}\lambda_j(\mathbf{R}_r)\right]^{\frac{1}{r(\mathbf{R}_r)}}\left(4\frac{r}{N}\frac{E_b}{N_0}\right)\right\}^{-r(\mathbf{R}_t)r(\mathbf{R}_r)d}. \end{aligned} \tag{4.12}$$

Therefore, for combined CC and orthogonal STBC, the diversity in the joint transmit-receive correlation case is $r(\mathbf{R}_t)r(\mathbf{R}_r)d_{\min}$. Similar to the STBC-only case discussed

in the previous section, assuming that the correlation matrices are full rank, the loss in coding gain due to correlation is the same as that shown in (4.8).

4.4 Performance Bounds of the Antenna Selection System over Correlated Channels

In this section, we derive upper bounds on the BER performance for the above systems with antenna selection. That is, the case when the receiver uses only L out of the available M receive antennas,where $1 \leq L \leq M$. Note that there are $\binom{M}{L}$ subsets to choose from, but we assume here that the selected subset is the one that results in the maximum SNR at the receiver.

4.4.1 Orthogonal STBC-Only System

Without loss of generality, we can assume that

$$\sum_{i=1}^{N} |\alpha_{1,i}|^2 \leq \sum_{i=1}^{N} |\alpha_{2,i}|^2 \leq \cdots \leq \sum_{i=1}^{N} |\alpha_{M,i}|^2 .$$

By knowing that the sum of the largest L out of M nonnegative numbers is always greater than or equal to the average of these M numbers multiplied by L, we have

$$\frac{L}{M} \sum_{j=1}^{M} \sum_{i=1}^{N} |\alpha_{j,i}|^2 \leq \sum_{j=M-L+1}^{M} \sum_{i=1}^{N} |\alpha_{j,i}|^2 . \tag{4.13}$$

By choosing the largest L terms in the sequence $\sum_{i=1}^{N} |\alpha_{j,i}|^2, j = 1, 2, \ldots, M$, the conditional BER, conditioned on the channel gain, can then be upper bounded as

$$P_b(e \mid \boldsymbol{\alpha}) \leq Q\left(\sqrt{2\frac{L}{M}\frac{E_s}{N_0}\sum_{j=1}^{M}\sum_{i=1}^{N}|\alpha_{j,i}|^2}\right). \tag{4.14}$$

By comparing the right-hand side of the expression in (4.14) with that in (4.2), we notice that both are the same except that the SNR in the former expression is scaled by L/M. Therefore the average BER performance, with antenna selection, will have a similar expression as that for the full-complexity system, namely

$$P_b(e) = \frac{1}{\pi}\int_0^{\pi/2}\prod_{i=1}^{r(\mathbf{R}_t)}\prod_{j=1}^{r(\mathbf{R}_r)}\left[1+\frac{L}{M}\frac{E_s}{N_0}\frac{1}{\sin^2\theta}\lambda_i(\mathbf{R}_t)\lambda_j(\mathbf{R}_r)\right]^{-1} d\theta. \tag{4.15}$$

At high SNR, (4.15) can be approximated as

$$\begin{aligned} P_b(e) \approx & \binom{2r(\mathbf{R}_t)r(\mathbf{R}_r)-1}{r(\mathbf{R}_t)r(\mathbf{R}_r)}\left\{\left[\prod_{i=1}^{r(\mathbf{R}_t)}\lambda_i(\mathbf{R}_t)\right]^{\frac{1}{r(\mathbf{R}_t)}}\right. \\ & \left.\cdot\left[\prod_{j=1}^{r(\mathbf{R}_r)}\lambda_j(\mathbf{R}_r)\right]^{\frac{1}{r(\mathbf{R}_r)}}\left(4\frac{L}{M}\frac{E_s}{N_0}\right)\right\}^{-r(\mathbf{R}_t)r(\mathbf{R}_r)}. \end{aligned} \tag{4.16}$$

This expression suggests that the diversity order with antenna selection is the same as that of the full complexity system, whereas the loss in coding gain is upper bounded by $10\log_{10}(M/L)$ dB.

4.4.2 Combined CC and Orthogonal STBC System

We can assume without loss of generality that at a certain time index n,

$$\sum_{i=1}^{N} |\alpha_{n,1,i}|^2 \leq \sum_{i=1}^{N} |\alpha_{n,2,i}|^2 \leq \cdots \leq \sum_{i=1}^{N} |\alpha_{n,M,i}|^2 .$$

Consequently, we have

$$\frac{L}{M} \sum_{j=1}^{M} \sum_{i=1}^{N} |\alpha_{n,j,i}|^2 \leq \sum_{j=M-L+1}^{M} \sum_{i=1}^{N} |\alpha_{n,j,i}|^2 . \tag{4.17}$$

By choosing the largest L terms in the sequence $\sum_{i=1}^{N} |\alpha_{n,j,i}|^2 , j = 1, 2, \ldots , M$, at each time index n, the conditional pairwise error probability, conditioned on the channel gain, can be upper bounded as

$$P_2 (d \,|\, \boldsymbol{\alpha}) \leq Q \left(\sqrt{2 \frac{r}{N} \frac{L}{M} \frac{E_b}{N_0} \sum_{n=1}^{d} \sum_{j=1}^{M} \sum_{i=1}^{N} |\alpha_{n,j,i}|^2} \right) .$$

The average pairwise error probability, with antenna selection will also have a similar expression as that for full-complexity system, namely

$$P_2 (d) = \frac{1}{\pi} \int_0^{\pi/2} \prod_{i=1}^{r(\mathbf{R}_t)} \prod_{j=1}^{r(\mathbf{R}_r)} \left[1 + \frac{r}{N} \frac{L}{M} \frac{E_b}{N_0} \frac{1}{\sin^2 \theta} \lambda_i (\mathbf{R}_t) \lambda_j (\mathbf{R}_r) \right]^{-d} d\theta. \tag{4.18}$$

As for the BER, it can also be upper bounded by using the expression in (4.11) with

$P_2(d)$ replaced by its expression in (4.18).

At high SNR, (4.18) can be approximated as

$$P_2(d) \approx \binom{2r(\mathbf{R}_t)r(\mathbf{R}_r)d-1}{r(\mathbf{R}_t)r(\mathbf{R}_r)d} \left\{ \left[\prod_{i=1}^{r(\mathbf{R}_t)} \lambda_i(\mathbf{R}_t) \right]^{\frac{1}{r(\mathbf{R}_t)}} \cdot \left[\prod_{j=1}^{r(\mathbf{R}_r)} \lambda_j(\mathbf{R}_r) \right]^{\frac{1}{r(\mathbf{R}_r)}} \left(4\frac{r}{N}\frac{L}{M}\frac{E_b}{N_0} \right) \right\}^{-r(\mathbf{R}_t)r(\mathbf{R}_r)d}. \quad (4.19)$$

By comparing (4.12) with (4.19), it is obvious that the diversity order is maintained with antenna selection as that of the full-complexity system for any $L \leq M$, and the reduction in SNR due to antenna selection is upper bounded by $10\log_{10}(M/L)$ dB.

4.5 Simulation and Numerical Results

Figs. 4.1 and 4.2 show the BER performance of the full-complexity system over various transmit correlation only channel. In Fig. 4.1, we consider the STBC-only system. The underlying transmit correlation matrices and their corresponding eigenvalues are

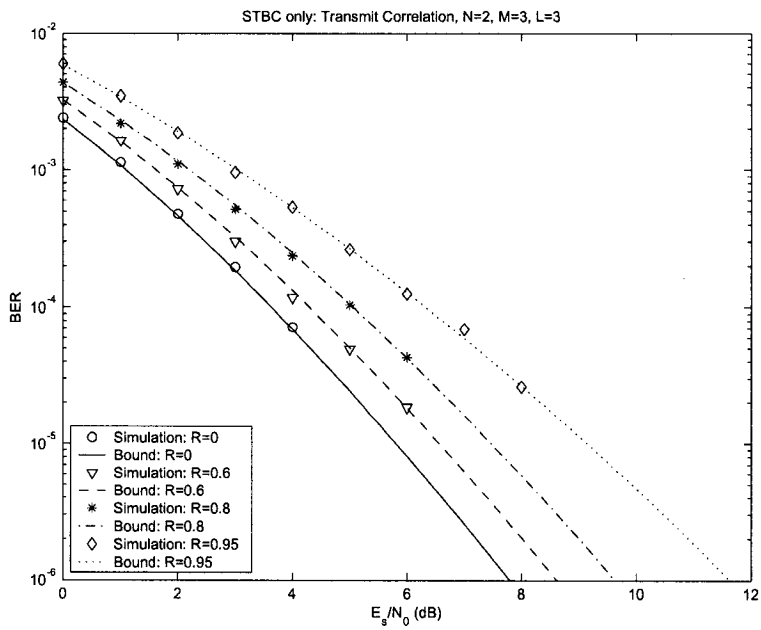

Figure 4.1: BER performance comparison of the full-complexity system over various transmit correlated channel for $N = 2, M = 3$ along with their exact bounds (STBCs only).

listed as follows.

$$\mathbf{R}_t^1 = \begin{bmatrix} 1 & 0 \\ 0 & 1 \end{bmatrix}, \text{ with } \lambda_1 = 1,\ \lambda_2 = 1$$

$$\mathbf{R}_t^2 = \begin{bmatrix} 1 & 0.6 \\ 0.6 & 1 \end{bmatrix}, \text{ with } \lambda_1 = 1.6,\ \lambda_2 = 0.4$$

$$\mathbf{R}_t^3 = \begin{bmatrix} 1 & 0.8 \\ 0.8 & 1 \end{bmatrix}, \text{ with } \lambda_1 = 1.8,\ \lambda_2 = 0.2$$

$$\mathbf{R}_t^4 = \begin{bmatrix} 1 & 0.95 \\ 0.95 & 1 \end{bmatrix}, \text{ with } \lambda_1 = 1.95,\ \lambda_2 = 0.05$$

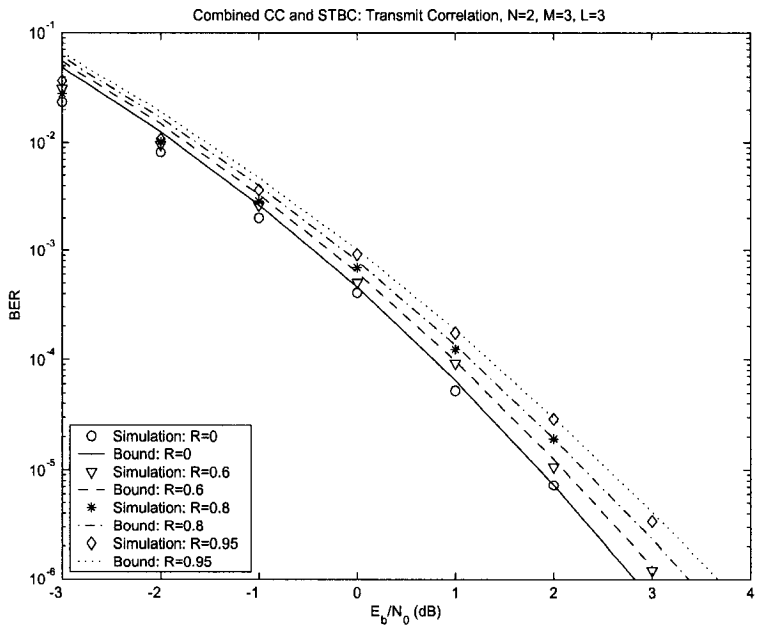

Figure 4.2: BER performance comparison of the full-complexity system over various transmit correlated channel for $N = 2, M = 3$ along with their transfer function bounds (Combined CC and STBCs).

Note that $\mathbf{R}_t^1$ is an identity matrix, which represents the correlation matrix of the independent fading channel. Whereas $\mathbf{R}_t^2$, $\mathbf{R}_t^3$, $\mathbf{R}_t^4$ represent the correlation matrix of the fading channels with transmit correlation, but they are all full rank. We can observe that the BER performance curve corresponding to $\mathbf{R}_t^2$ has the same slope as that corresponding to $\mathbf{R}_t^1$ at high SNR, and the loss of the coding gain due to transmit correlation is about $10\log_{10}(1.6 \times 0.4)^{-1/2} = 0.97$ dB relative to the independent channels. However, this observation is not straightforward for the curves corresponding to $\mathbf{R}_t^3$ and $\mathbf{R}_t^4$. This is simply because the SNR we considered for simulation purposes is not high enough.

In Fig. 4.2, we consider the combined CC and STBC system. On the same figure,

we plot the performance bounds using (4.10) and (4.11) (only the first 5 terms in the sum are considered). The observation is the same as that for Fig. 4.1. Furthermore, by comparing Figs. 4.1 and 4.2, we can observe that this combined coding scheme provides more diversity order compared with that of the STBC-only scheme.

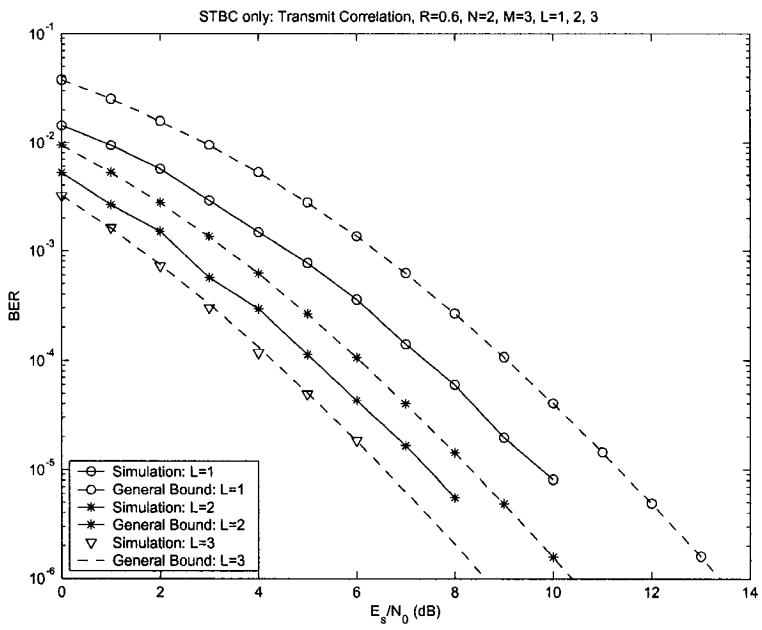

Figure 4.3: BER performance comparison between various antenna selection scenarios over transmit correlated channel for $N = 2, M = 3$ along with their upper bounds (STBCs only).

In Figs. 4.3 and 4.4, we plot the simulation results and the general bounds for antenna selection system over transmit correlation only channel with transmit correlation matrix $\mathbf{R}_t^2$. It is clear from each of the figures that all curves have the same slope, suggesting that they have the same diversity order as that of the full complexity system, which agrees with our analysis above. Moreover, for the STBC-only system, the loss in SNR due to antenna selection for $L = 2$ and $L = 1$ are about 0.4 dB and

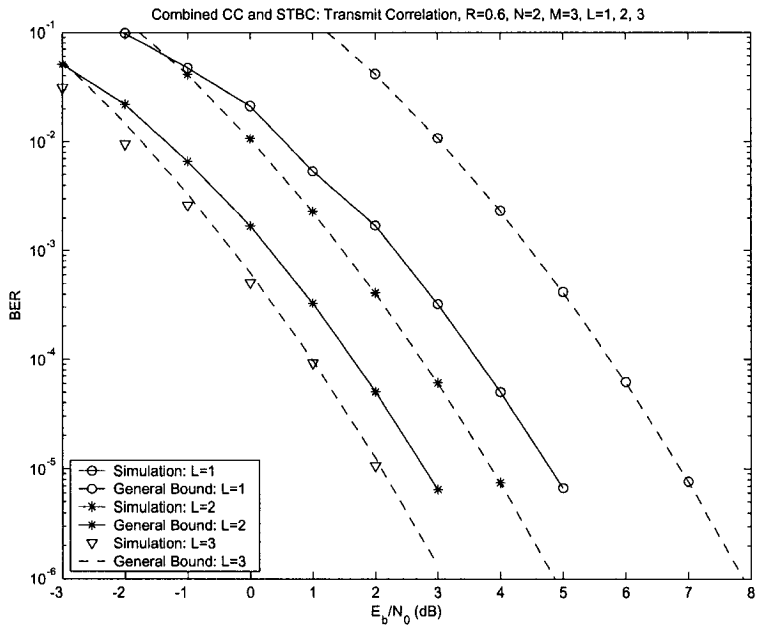

Figure 4.4: BER performance comparison between various antenna selection scenarios over transmit correlated channel for $N = 2, M = 3$ along with their upper bounds (Combined CC and STBCs).

3.5 dB at $P_b = 10^{-5}$, respectively, relative to the case $L = 3$ (i.e., no selection). For the combined CC and STBC system, the corresponding loss in SNR due to antenna selection are about 0.4 dB and 2.5 dB respectively. These losses are smaller than their upper bounds (i.e., $10\log_{10}(3/2) = 1.76$ and $10\log_{10}(3) = 4.77$ dB.) We point out here that the gap between this bound and simulations gets smaller as L approaches M. This is simply because the approximation we used in (4.13) and (4.17) becomes more accurate as L increases.

We repeat the above experiment for the receive correlation only scenario and joint transmit-receive correlation scenario. In Figs. 4.5 and 4.6, we plot the simulation results and the general bounds for the antenna selection system over receive correlation

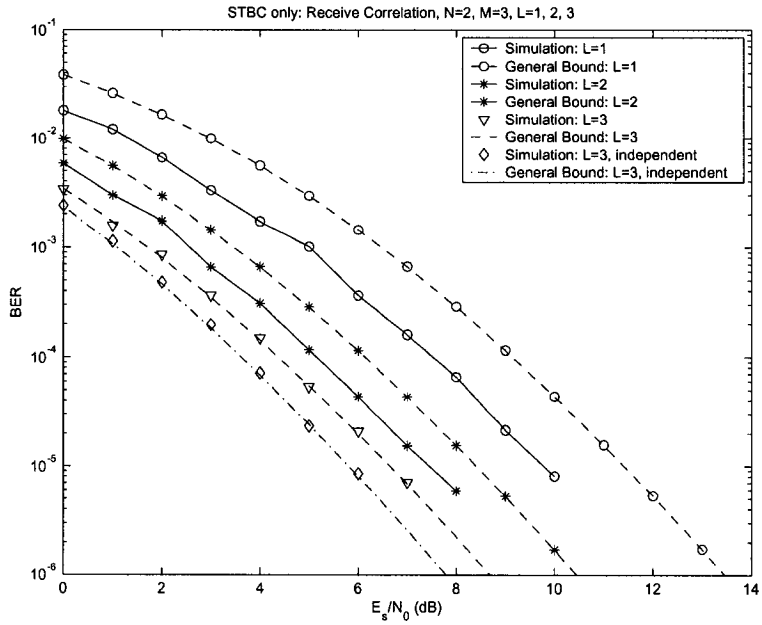

Figure 4.5: BER performance comparison between various antenna selection scenarios over receive correlated channel for $N = 2, M = 3$ along with their upper bounds (STBCs only).

only channel with receive correlation matrix

$$\mathbf{R}_r^1 = \begin{bmatrix} 1 & 0.6 & 0.4 \\ 0.6 & 1 & 0.45 \\ 0.4 & 0.45 & 1 \end{bmatrix},$$

where the eigenvalues are $\lambda_1 = 1.9720$, $\lambda_2 = 0.6321$, $\lambda_3 = 0.3959$. In Fig. 4.5, we consider the STBC-only system. It is easy to observe that the BER curve of the full-complexity system over the correlated channel has the same slope as that of the independent channel and the loss of the coding gain is about $10\log_{10}(1.9720 \times 0.6321 \times 0.3959)^{-1/3} = 1.02$ dB relative to the independent channels at high SNR.

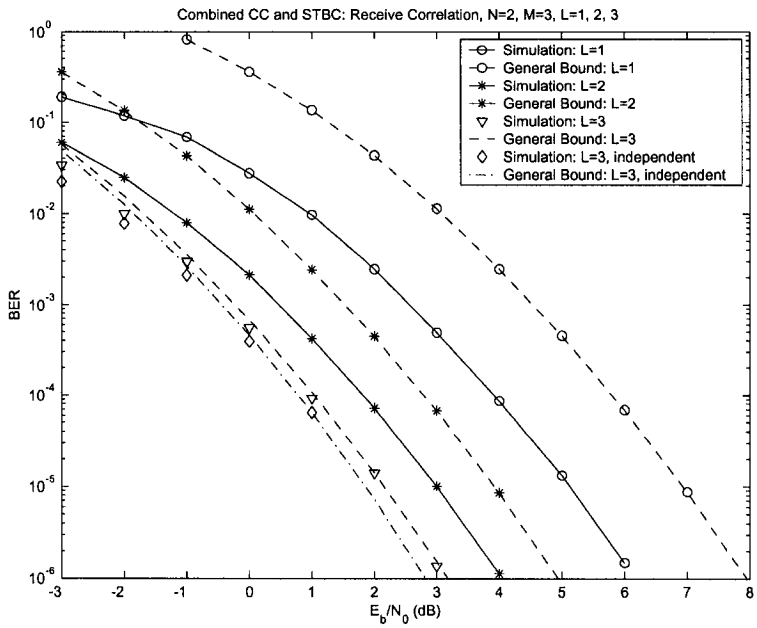

Figure 4.6: BER performance comparison between various antenna selection scenarios over receive correlated channel for $N = 2, M = 3$ along with their upper bounds (Combined CC and STBCs).

We also observe that all the curves have the same slope. It suggests again that the diversity order is maintained with antenna selection and the loss in SNR due to antenna selection is upper bounded by $10\log_{10}(M/L)$ dB. In Fig. 4.6, combined CC and STBC system is considered over receive correlation only channel with receive antenna selection and we can have the same observation as that for Fig. 4.5.

In Figs. 4.7 and 4.8, we plot the simulation results and the general bounds for the antenna selection system over joint transmit-receive correlation fading channels with transmit correlation matrix $\mathbf{R}_t^2$ and receive correlation matrix $\mathbf{R}_r^1$. In Fig. 4.7, we consider the STBC-only system. It is easy to observe that the BER curve of the full-complexity system over the correlated channels has the same slope

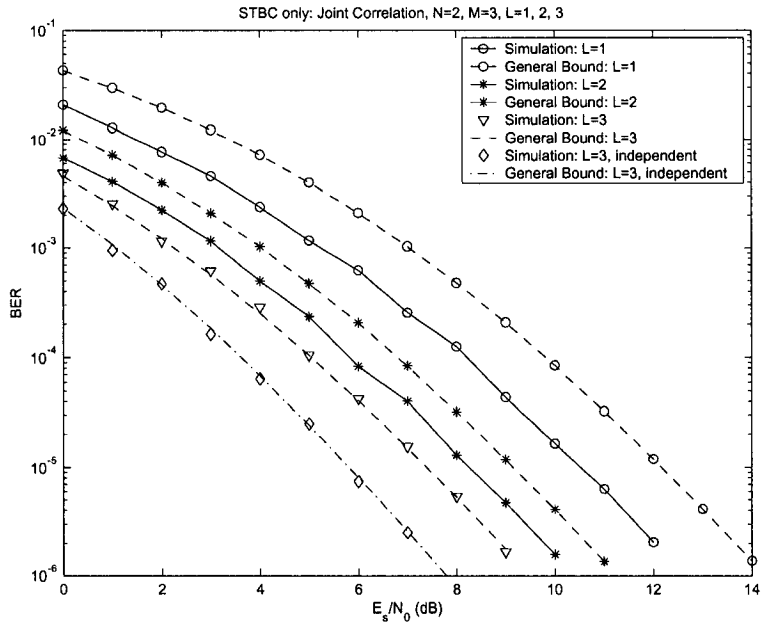

Figure 4.7: BER performance comparison between various antenna selection scenarios over joint correlated channel for $N = 2, M = 3$ along with their upper bounds (STBCs only).

as that over the independent channels, and the loss of the coding gain is about $10\log_{10}\left[(1.6\times 0.4)^{-1/2}\times(1.9720\times 0.6321\times 0.3959)^{-1/3}\right] = 1.99$ dB relative to the independent channels. We also observe that all the curves have the same slope. It suggests again that the diversity order is maintained with antenna selection and the loss in SNR due to antenna selection is upper bounded by $10\log_{10}(M/L)$ dB. In Fig. 4.8, combined CC and STBC system is considered over joint transmit-receive correlation channel with receive antenna selection and we can have the same observation.

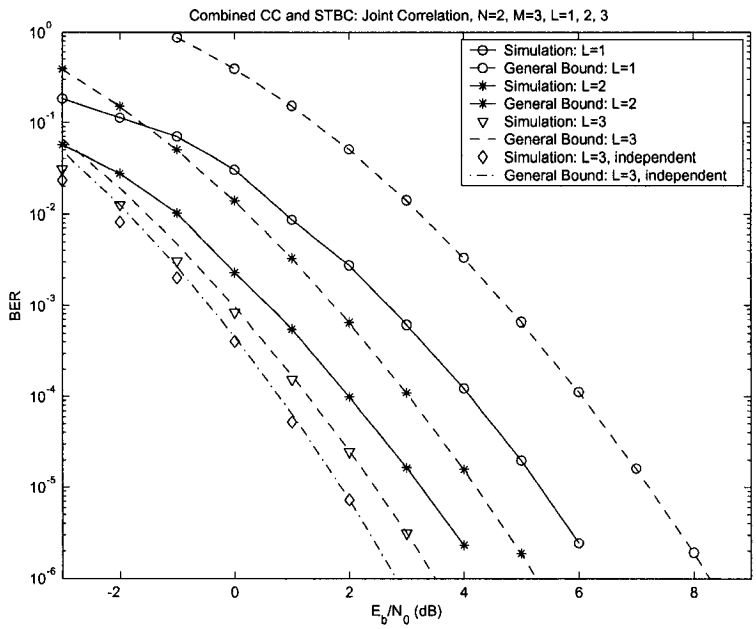

Figure 4.8: BER performance comparison between various antenna selection scenarios over joint correlated channel for $N = 2, M = 3$ along with their upper bounds (Combined CC and STBCs).

4.6 Conclusions

In this chapter, we analyzed the performance of combined convolutional coding and orthogonal space-time block coding with receive antenna selection in correlated fading channel. We used a pragmatic selection criterion that maximizes the SNR at the receiver. We derived an upper bound, which explicitly showed that the diversity order with antenna selection is maintained as that of the full-complexity system, whereas the coding gain deteriorates by a value upper bounded by $10\log_{10}(M/L)$ dB. We also quantified the loss in coding gain due to spatial correlation, provided that the correlation matrices are full rank. We also presented several examples through which

we validated our analytical results. The analysis used in this chapter can be easily applied to the combined TCM and STBC in the face of antenna selection.

Chapter 5

Conclusions and Future Work

5.1 Conclusions

In this thesis, we present a comprehensive performance analysis of the receive antenna selection for MIMO systems. We considered STBC-only systems, and the combined outer channel coding with STBC systems over independent and correlated Rayleigh flat fading channel respectively. At last, we get a conclusion which can be applied to all of these scenarios that the antenna diversity gain is maintained with receive antenna selection for any number of selected antennas, whereas the SNR deterioration due to antenna selection can be upper bounded by $10\log_{10}(M/L)$ dB. So, the receive antenna selection is an effective scheme for reducing hardware complexity in MIMO system.

5.2 Future Work

- The next step in our work is to study the antenna selection at the transmitter side based on full or limited channel information fed back by the receiver. In practice, the feedback channel has a very limited capacity. Typically, only a few bits are reserved for control purposes. So, the limited feedback information is especially attractive in that they allow antenna selection at the transmitter without requiring a full description of the channel to be fed back. In particular, the only information fed back is the selected subset of antennas to be employed. We will consider two different transmit antenna selection criterion for two kinds of channels. For slow fading channel, the antenna selection can be carried out based on channel state information. we select those transmit antennas which maximize the instantaneous SNR by comparing the channel magnitude for each transmit antennas. However, if the channel state changes fast, due to the delay and limited capacity of feedback channel, it may be impossible to perform transmit antenna selection every time the channel changes. In this case, we can perform transmit antenna selection every time the second order channel statistic changes. That is, we can select those antennas which minimize the average error probability based on the channel covariance matrix. After this, we shall consider the joint transmit-receive antenna selection scheme.

- Modify the system model to take the channel estimation error into consideration. The channel fading coefficients are estimated by inserting pilot sequences

in the transmitted signals. Assume channel is constant over the duration of a frame and independent between the frames. At the beginning of each frame, orthogonal pilot sequences are transmitted form each transmit antennas. Then the receiver estimates the channel fading coefficients by using the minimum mean square error (MMSE) algorithm. It has been shown that with MMSE, the estimation error due to noise can be modeled as a zero mean complex Gaussian random variable. We will investigate the sensitivity of antenna selection to channel estimation error. The error may also happen to the control bits of the feedback channel. By knowing the error probability of each control bit, we can also quantify the impact of feedback channel error to the transmit antenna selection.

- We only investigate the antenna selection over flat fading channel in our work. However, for high data rate wireless communication systems, such as W-CDMA system, the signal duration may be small compared to the multipath spread of the channel, resulting in a frequency-selective fading channel or equivalently a temporal ISI channel. So, the study of antenna selection technique over frequency-selective fading channels needs to be done. In this case, antenna selection is carried out by comparing the average energy contained in the multiple paths corresponding to each antenna. Furthermore, because of the multiple paths, at the receiver the orthogonality of STBC does not hold any more. Consequently, a equalizer should be employed to convert the channel into a temporal ISI-free channel. So, the orthogonality between signals after the equalizer still

holds, and the ML can be realized by simple linear processing.

- A more attractive but tough job is to apply the antenna selection technique in cooperative wireless network. In the relay channel, suppose data is to be transmitted from the source terminal S to destination terminal D. Due to the broadcast channel, another terminal in the network which we denote as the relay terminal R, also receive the signal from S and thus can cooperate with S to accomplish the communication with D. In this case, the antenna on S and that on R form a virtual transmit antenna array which realizes spatial diversity gain in a distributed fashion, but the delay between the received signal copies at D due to processing delay at R need be taken into the consideration for transmit antenna selection this time.

Appendix A

Component Codes Used in Simulation

A.1 Orthogonal STBCs for Three Transmit Antennas

The transmission matrix of full rate STBC for real signal constellation set is given by [6]

$$\mathbf{X}_3 = \begin{bmatrix} x_1 & -x_2 & -x_3 & -x_4 \\ x_2 & x_1 & x_4 & -x_3 \\ x_3 & -x_4 & x_1 & x_2 \end{bmatrix}. \tag{A.1}$$

The transmission matrix of rate 3/4 STBC for complex signal constellation set is given as follows. [57]

$$\mathbf{X}_3 = \begin{bmatrix} x_1 & x_2^* & x_3^* & 0 \\ -x_2 & x_1^* & 0 & -x_3^* \\ -x_3 & 0 & x_1^* & x_2^* \end{bmatrix} \tag{A.2}$$

A.2 Rate 1/2 $(7,5)_{oct}$ CC Code

The encoder diagram of $(7,5)_{oct}$ CC is shown in Fig. A.1. At each instant, the encoder accepts 1 input bit and outputs 2 coded bits. The constrain length is 3.

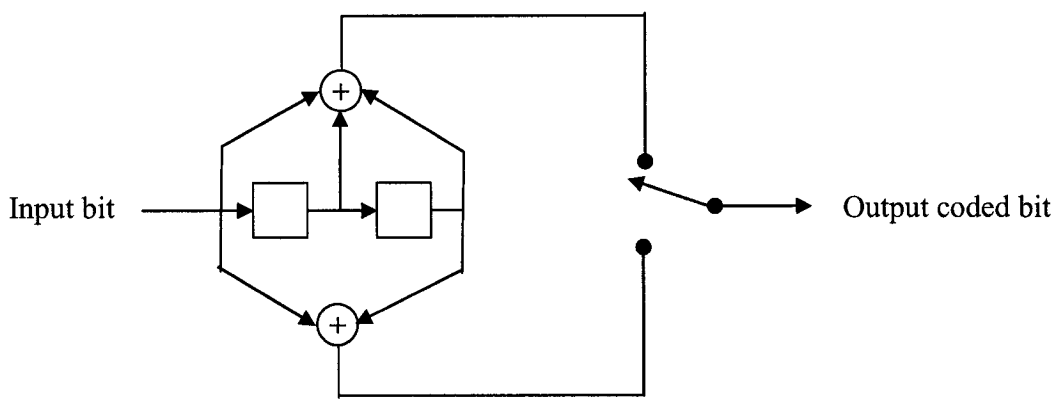

Figure A.1: $(7,5)_{oct}$ CC encoder.

It's transfer function is given by

$$\begin{aligned} T(D,N,J) &= \frac{J^3ND^5}{1-JND-J^2ND} \\ &= J^3ND^5 + \left(J^4+J^5\right)N^2D^6 + \left(J^5+2J^6+J^7\right)N^3D^7 + \cdots \end{aligned}$$

It means there are 2^l paths of distance $l+5$ from the all-zeros path and of $l+1$ 1s in the information sequence of that path, where $l = 0, 1, 2, \cdots$. The free distance is 5.

A.3 4-state, 8−PSK TCM Code

For Rayleigh fading channel, Wilson suggest a 4-state, 8−PSK TCM without parallel transmissions. The trellis diagram of this code and 8-PSK signal set are shown in Fig. A.2. As is shown, the trellis diagram of this code is fully connected and results in shortest error event paths of length two. This is the maximum achievable time diversity with 4-state TCM scheme.

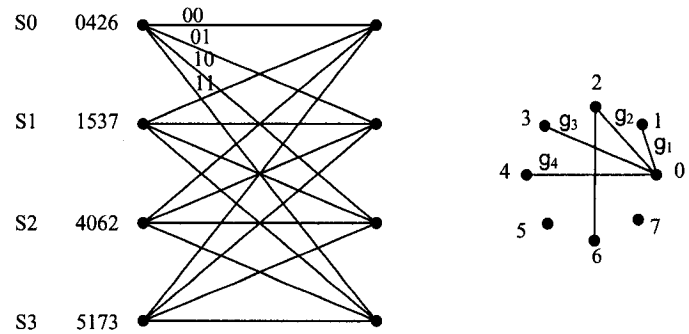

Figure A.2: 4-state, 8−PSK TCM code trellis diagram and signal set.

The labels listed left to a state node indicates the branch labels for transitions from that state corresponding to the encoder inputs 00, 01, 10, and 11 respectively. $g_1^2 = 0.586$, $g_2^2 = 2$, $g_3^2 = 3.414$, and $g_4^2 = 4$, represent the square of the normalized Euclidean distance between signals in the constellation set. Since this code is linear, its transfer function can be obtained from the modified error state transition diagram

as shown in Fig. A.3.

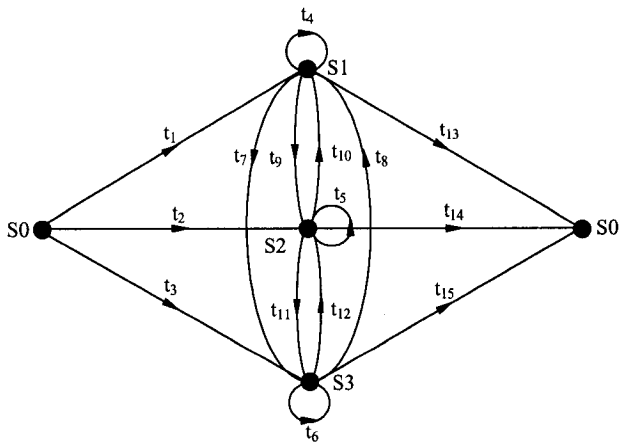

Figure A.3: Modified error state diagram of the 4-state, 8−PSK TCM code

The transfer function can be shown to be

$$T(D, I) = \xi_1 t_{13} + \xi_2 t_{14} + \xi_3 t_{15} \tag{A.3}$$

where,

$$\begin{bmatrix} \xi_1 \\ \xi_2 \\ \xi_3 \end{bmatrix} = \begin{bmatrix} 1 - t_4 & -t_{10} & -t_8 \\ -t_9 & 1 - t_5 & -t_{12} \\ -t_7 & -t_{11} & 1 - t_6 \end{bmatrix}^{-1} \begin{bmatrix} t_1 \\ t_2 \\ t_3 \end{bmatrix}.$$

We list the branch labels used for evaluating of the performance over AWGN channel, and MIMO Rayleigh fading channel respectively in the following table.

Branch Label	AWGN channel $\left(D = exp(-\frac{E_s}{4N_0}\frac{1}{\sin^2\theta})\right)$	MIMO Rayleigh fading channel $\left(D = \frac{1}{N}\frac{E_s}{4N_0}\frac{1}{\sin^2\theta}\right)$
t_1	$ID^{g_4^2}$	$I\left(1+Dg_4^2\right)^{-NM}$
t_2	$ID^{g_2^2}$	$I\left(1+Dg_2^2\right)^{-NM}$
t_3	$I^2D^{g_2^2}$	$I^2\left(1+Dg_2^2\right)^{-NM}$
t_4	$ID^{g_3^2}$	$I\left(1+Dg_3^2\right)^{-NM}$
t_5	$ID^{g_2^2}$	$I\left(1+Dg_2^2\right)^{-NM}$
t_6	$\frac{1}{2}I^2\left(D^{g_1^2}+D^{g_3^2}\right)$	$\frac{1}{2}I^2\left(\left(1+Dg_1^2\right)^{-NM}+\left(1+Dg_3^2\right)^{-NM}\right)$
t_7	$\frac{1}{2}I^2\left(D^{g_1^2}+D^{g_3^2}\right)$	$\frac{1}{2}I^2\left(\left(1+Dg_1^2\right)^{-NM}+\left(1+Dg_3^2\right)^{-NM}\right)$
t_8	$ID^{g_1^2}$	$I\left(1+Dg_1^2\right)^{-NM}$
t_9	$\frac{1}{2}I\left(D^{g_1^2}+D^{g_3^2}\right)$	$\frac{1}{2}I\left(\left(1+Dg_1^2\right)^{-NM}+\left(1+Dg_3^2\right)^{-NM}\right)$
t_{10}	ID	$I\left(1+D\right)^{-NM}$
t_{11}	$I^2D^{g_2^2}$	$I^2\left(1+Dg_2^2\right)^{-NM}$
t_{12}	$\frac{1}{2}I\left(D^{g_1^2}+D^{g_3^2}\right)$	$\frac{1}{2}I\left(\left(1+Dg_1^2\right)^{-NM}+\left(1+Dg_3^2\right)^{-NM}\right)$
t_{13}	$D^{g_1^2}$	$\left(1+Dg_1^2\right)^{-NM}$
t_{14}	$D^{g_4^2}$	$\left(1+Dg_4^2\right)^{-NM}$
t_{15}	$D^{g_3^2}$	$\left(1+Dg_3^2\right)^{-NM}$

Table A.1: Branch labels of the modified error state diagram of the 4-state, 8−PSK TCM code.

Appendix B

The Definite Integration Used in the Derivation

1. $\int_0^\infty x^n e^{-ax} dx = \frac{n!}{a^{n+1}}$
2. $\int_0^\infty x^n e^{-r^2 x^2} dx = \frac{\Gamma[(n+1)/2]}{2r^{n+1}}$
3. $\frac{1}{\pi} \int_0^\infty \frac{1}{(x^2+1)^{L+1}} dx = \frac{1}{4^L} \binom{2L-1}{L}$
4. $\int_0^\infty Q\left(\sqrt{ax}\right) x^n e^{-x} dx = \frac{n!}{2} \left(1 - \sqrt{\frac{a}{2\pi}} \sum_{k=0}^{n} \frac{\Gamma(k+\frac{1}{2})}{k!(1+\frac{a}{2})^{k+1/2}}\right), a \geq 0$

This integration can be evaluated as follows. As we know that

$$\int x^n e^{-x} dx = -\sum_{k=0}^{n} \frac{n!}{k!} x^k e^{-x},$$

so we have

$$\begin{aligned}\int_0^\infty Q\left(\sqrt{ax}\right)x^n e^{-x}dx &= -\int_0^\infty Q\left(\sqrt{ax}\right)d\left(\sum_{k=0}^{n}\frac{n!}{k!}x^k e^{-x}\right)\\ &= \left[-Q\left(\sqrt{ax}\right)\sum_{k=0}^{n}\frac{n!}{k!}x^k e^{-x}\right]_0^\infty + \int_0^\infty \sum_{k=0}^{n}\frac{n!}{k!}x^k e^{-x}d\left(Q\left(\sqrt{ax}\right)\right)\\ &= \frac{n!}{2}+\sum_{k=0}^{n}\frac{n!}{k!}\int_0^\infty x^k e^{-x}d\left(Q\left(\sqrt{ax}\right)\right).\end{aligned}$$

Assume $y=\sqrt{ax}$, the last line of above equation can be represented as

$$\int_0^\infty Q\left(\sqrt{ax}\right)x^n e^{-x}dx = \frac{n!}{2}+\sum_{k=0}^{n}\frac{n!}{k!a^k}\int_0^\infty y^{2k}e^{-\frac{1}{a}y^2}dQ\left(y\right).$$

According to the definition of $Q\left(y\right)$, we have $dQ\left(y\right)=-\frac{1}{\sqrt{2\pi}}e^{-y^2/2}dy$, so

$$\int_0^\infty Q\left(\sqrt{ax}\right)x^n e^{-x}dx = \frac{n!}{2}-\sum_{k=0}^{n}\frac{n!}{k!a^k\sqrt{2\pi}}\int_0^\infty y^{2k}e^{-\frac{1+a/2}{a}y^2}dy.$$

By knowing that $\int_0^\infty x^n e^{-r^2x^2}dx=\frac{\Gamma[(n+1)/2]}{2r^{n+1}}$, after some algebraic manipulations, we can get the final result as shown above.

5. $\int_{-1}^{1}\frac{f(x)}{\sqrt{1-x^2}}dx=\sum_{i=1}^{n}w_i f\left(x_i\right)+R_n$

Where, $x_i=\cos\frac{(2i-1)\pi}{2n}$, $w_i=\frac{\pi}{n}$, and remainder $R_n=\frac{\pi}{(2n)!2^{2n-1}}f^{(2n)}\left(\xi\right)$ $(-1<\xi<1)$. As n increase the remainder term R_n becomes negligible [58] (25.4.38).

Bibliography

[1] E. Telatar, "Capacity of multi-antenna Gaussian channels," *AT&T Bell Labs Internal Memo.*, June 1995.

[2] G. Foschini and M. Gans, "On the limits of wireless communications in a fading environment when using multiple antenna," *Wireless Personal Commun.*, vol. 6, no. 3, pp. 311-335, March 1998.

[3] J. C. Guey, M. P. Fitz, M. R. Bell, and W. Y. Kuo, "Signal design for transmitter diversity wireless communication systems over Rayleigh fading channels," *Proc., IEEE Veh. Tech. Conf. (VTC),* vol. 1, pp. 136-140, 1996.

[4] V. Tarokh, N. Seshadri, and A. R. Calderbank, "Space-time codes for high data rate wireless communication: Performance criterion and code construction," *IEEE Trans. Info. Theory,* vol. 44, pp. 744-765, March 1998.

[5] S. M. Alamouti, "A simple transmit diversity technique for wireless communications," *IEEE J. on Selected Areas in Commun.,* vol.16, No. 8, pp. 1451-1458, Oct. 1998.

[6] V. Tarokh, H. Jafarkhani, and A. R. Calderbank, "Space-time block codes from orthogonal designs," *IEEE Trans. Info. Theory,* vol. 45, no. 5, pp. 1456-1467, July 1999.

[7] A. R. Hammons, Jr. and H. El Gamal, "On the theory of space-time codes for PSK modulation," *IEEE Trans. Info. Theory,* vol. 46, no. 2, pp. 524-542, March 2000.

[8] Q. Yan and R. S. Blum, "Optimum space-time convolutional codes," *Proc., IEEE Wireless Commun. and Net. Conf. (WCNC),* vol. 3, pp. 1351-1355, 2000.

[9] S. Baro, G. Bauch, and A. Hansmann, "Improved codes for space-time trellis-coded modulation," *IEEE Commu. Lett.,* vol. 4, no.1, pp. 20-22, January 2000.

[10] Y. Liu, M. P. Fitz, and O. Y. Takeshita, "Full rate space-time turbo codes," *IEEE J. on Selected Areas in Commun.,* vol. 19, no. 5, pp. 969-980, May 2001.

[11] A. Stefanov and T. M. Duman, "Turbo coded modulation for systems with transmit and receive antenna diversity over block fading channels: System model, decoding approaches and practical considerations," *IEEE J. of Selected Areas in Commun.,* vol. 19, no. 5, pp. 958-968, May 2001.

[12] G. Kang, X. Jin, Q. Quan, P. Zhang, "The decision schemes on the concatenation of space-time block code and convolutional code in WCDMA system," *International Conferences on Info-tech and Info-net,* vol. 2 , pp. 693 - 697, 29 Oct.-1 Nov. 2001.

[13] S. M. Alamouti, V. Tarokh, and P. Poon, "Trellis-coded modulation and transmit diversity: design criteria and performance evaluation," *Proc. IEEE Inter. Conf. on Universal Personal Commun. (ICUPC),* vol. 1, pp. 703-707, 1998.

[14] Y. Gong and K. B. Letaief, "Concatenated space-time block coding with trellis coded modulation in fading channels," *IEEE Trans. Wireless Commun.,* vol. 1, no. 4, pp. 580-590, Oct. 2002.

[15] A. Yongacoglu, and M. Siala, "Space-time codes for fading channels," *IEEE Trans. Veh. Technol.,* vol. 5, pp. 2495-2499, Sept. 1999.

[16] G. Bauch, "Concatenation of space-time block codes and "turbo"-TCM," *IEEE International Conference on Communications,* vol. 2, pp.1202-1206, June 1999.

[17] S. Sandhu, R. Heath, and A. Paulraj, "Space-time block codes versus space-time trellis codes," *Proc., IEEE Inter. Conf. on Commun. (ICC),* vol. 4, pp. 11-14, June 2001.

[18] D. Gore and A. Paulraj, "Statistical MIMO antenna sub-selection with space-time coding," *Proc., IEEE Inter. Conf. on Commun. (ICC),* vol. 1, pp. 641-645, 2002.

[19] D. Gore, R. U. Nabar, and A. Paulraj, "Selecting an optimal set of transmit antennas for a low rank matrix channel," *Proc., IEEE Inter. Conf. on Acous., Speech and Sig. Proc. (ICASSP),* pp. 2785-2788, 2000.

[20] R. W. Heath, S. Sandhu, and A. Paulraj, "Antenna selection for spatial multiplexing systems with linear receivers," *IEEE Commun. Lett.,* vol. 5, no. 4, pp. 142-144, April 2001.

[21] A. Ghrayeb and T. M. Duman, "Performance analysis of MIMO systems with antenna selection over quasi-static fading channels," *IEEE Trans. on Veh. Tech.,* vol. 52, no. 2, pp. 281-288, March 2003.

[22] A. Ghrayeb, A. Sanei, and Y. Shayan, "Space-time trellis codes with receive antenna selection in fast fading," *IEE Electronics Letters*, vol. 40, no. 10, pp. 613-614, May 2004.

[23] A. F. Molisch, M. Z. Win, and J. H. Winters, "Capacity of MIMO systems with antenna selection," *Proc., IEEE Inter. Conf. on Commun. (ICC),* vol. 2, pp. 570-574, June 2001.

[24] I. Bahceci, T. M. Duman, and Y. Altunbasak, "Antenna selection for multiple-antenna transmission systems: Performance analysis and code construction," *IEEE Trans. on Info. Theory,* vol. 49, no. 10, pp. 2669-2681, Oct. 2003.

[25] A. Gorokhov, D. A. Gore, and A. J. Paulraj, "Receive antenna selection for MIMO spatial multiplexing: theory and algorithms," *IEEE Trans. Sig. Proc.,* vol. 51, no. 11, pp. 2796-2807, Nov. 2003.

[26] A. Gorokhov, D. A. Gore, and A. J. Paulraj, "Receive antenna selection for MIMO flat-fading channels: theory and algorithms," *IEEE Trans. Info. Theory,* vol. 49, no. 10, pp. 2687-2696, Oct. 2003.

[27] C. Zhuo, B. Vucetic, and Y. Jinhong, "Space-time trellis codes with transmit antenna selection," *IEE Elect. Lett.,* vol. 39, no. 11, pp. 854-855, May 2003.

[28] A. F. Molisch and X. Zhang, "FFT-based hybrid antenna selection schemes for spatially correlated MIMO channels," *IEEE Commun. Lett.,* vol. 8, no. 1, pp. 36-38, Jan. 2004.

[29] R. S. Blum and J. H. Winters, "On optimum MIMO with antenna selection," *IEEE Commun. Lett.,* vol. 6, no. 8, pp. 322-324, Aug. 2002.

[30] R. S. Blum, "MIMO capacity with antenna selection and interference," *Proc. IEEE Inter. Conf. of Acous., Speech, and Sig. Proc. (ICASSP),* vol. 4, pp. 824-827, 2003.

[31] C. Zhuo, Y. Jinhong, B. Vucetic, and Z. Zhendong, "Performance of Alamouti scheme with transmit antenna selection," *IEE Elect. Lett.,* vol. 39, no. 23, pp. 1666-1668, Nov. 2003.

[32] H. W. Wing and E. G. Larsson, "Orthogonal space-time block coding with antenna selection and power allocation," *IEE Elect. Lett.,* vol. 39, no. 4, pp. 379-381, Feb. 2003.

[33] M. Katz, E. Tiirola, and J. Ylitalo, "Combining space-time block coding with diversity antenna selection for improved downlink performance," *Proc. IEEE Veh. Tech. Conf. (VTC),* pp. 178-182, 2001.

[34] D. A. Gore and A. Paulraj, "MIMO antenna subset selection with space-time coding," *IEEE Trans. on Sig. Proc.*, vol. 50, no. 10, pp. 2580-2588, Oct. 2002.

[35] W. Hamouda and A. Ghrayeb, "Performance of convolutionally-coded MIMO systems with antenna selection," *Proc., IEEE Veh. Tech. Conf. (VTC),* Milan, Italy, May 2004.

[36] T.S. Rappaport, *Wireless Communiation Principles and Practice*, Prentice-Hall, Inc, 1996.

[37] A. F. Molisch, M. Z. Win, and J. H. Winters, "Reduced-complexity transmit/receive-diversity systems," *IEEE Trans. Sig. Proc.*, vol. 51, no. 11, pp. 2729-2738, Nov. 2003.

[38] S. Thoen, L. V. der Perre, M. Engels, and B. Gyselinckx, "Performance analysis of combined transmit-SC/receive-MRC," *IEEE Trans. Commun.*, vol. 49, pp. 5-8, Jan. 2001.

[39] N. Kong and L. B. Milstein, "Combined average SNR of a generalized selection combining scheme," *Proc. IEEE International Conf. Commun.*, vol. 3, Atlanta, GA, June 1998, pp. 1556-1560.

[40] M. Z. Win and J. H. Winters, "Virtual branch analysis of symbol error probability for hybrid selection/maximal-ratio combining in Rayleigh fading," *IEEE Trans. Commun.*, vol. 49, pp. 1926-1934, Nov. 2001.

[41] M.-S. Alouini and M. K. Simon, "Performance of coherent receivers with hybrid SC/MRC over Nakagami-m fading channels," *IEEE Trans. Veh. Technol.*, vol. 48, pp. 1155-1164, July 1999.

[42] P. K. Mallik and M. Z. Win, "Analysis of hybrid selection/maximal-ratio combining in correlated Nakagami fading," *IEEE Trans. Commun.,* vol. 8, pp. 1372-1383, Aug. 2002.

[43] A. F. Molisch and M. Z. Win, "MIMO systems with antenna selection," *IEEE Microwave Magazine*, pp. 46-56, March 2004.

[44] C.-N. Chuah, D. Tse, J. Kahn, and R. Valenzuela, "Capacity scaling in MIMO wireless systems under correlated fading," *IEEE Transactions on Information Theory,* Vol. 48, No. 3, March 2002.

[45] Michel T. Ivrlac, Wolfgang Utschick, Josef A. Nossek, "Fading correlations in wireless MIMO communication systems," *IEEE Journal on Selected Areas in Communications,* no. 5, pp. 819-828, Jun 2003.

[46] H. Bölcskei and A. J. Paulraj, "Performance of space-time codes in the presence of spatial fading correlation," *Asilomar Conf. on Signals, Systems, and Computers,* Pacific Grove, CA, Oct. 2000.

[47] H. Shah, A. Hedayat, and A. Nosratinia, "Performance of concatenated channel codes and orthogonal space-time block codes," *IEEE Transaction on Wireless*, submitted for publication.

[48] I. Bahceci, Y. Altunbasak and T. M. Duman, "Space-time coding over correlated fading channels with antenna selection," *IEEE Inter. Conf. on Commun. (ICC),* vol. 2, pp. 832-836, June 2004.

[49] J. G. Proakis, *Digital Communications*, 4^{th} Ed., McGraw Hill, 2000.

[50] B. C. Arnold, N. Balakrishnan, and H. N. Nagaraja, *A First Course in Order Statistics*, Wiley-Inetrscience, 1993.

[51] E. Biglieri, D. Divsalar, P. J. MaLane, and M. K. Simon, *Introduction to Trellis-Coded Modulation with Applications,* Macmillan, 1991.

[52] J. W. Craig, "A new, simple and exact result for calculating the probability of error for two-dimensional signal constellations," *IEEE MILCOM Conf.* Rec., vol. 2, pp. 571-575, McLean, VA, Oct. 1991.

[53] G. Femenias, and I. Furio, "A new, simple, and exact union bound for reference-based predetection and postdetection diversity TCM-MPSK systems in Rayleigh fading," *IEEE Trans. Veh. Technol.*, vol. 49, no. 2, pp. 540-549, Mar 2000.

[54] C. Tellambura, "Evaluation of the exact union bound for trellis-coded modulation over fading channels," *IEEE Trans. on Commun.*, vol. 44, no. 12, Dec. 1996.

[55] S. G. Wilson and Y. S. Leung, "Trellis-coded phase modulation on Rayleigh fading channels," *Proc. IEEE Inter. Conf. Commun. (ICC)* , pp. 21.3.1-21.3.5, June 1987.

[56] G. L. Turin, "The characteristic function of hermitian quadratic forms in complex normal variables," *Biometrika,* vol. 47, pp. 199–201, June 1960.

[57] B. Hochwald, T. L. Marzetta, C. B. Papadias, "A transmitter diversity scheme for wideband CDMA systems based on space-time spreading," *IEEE Journal on Selected Areas in Communications,* no. 1, pp. 48-60, January 2001.

[58] M. Abramowitz and I. A. Stegun, *Handbook of Mathematical Functions with Formulas, Graphs, and Mathematical Tables*, New York: Dover, 1964.